Russian Geology and Geophysics © 2022, Novosibirsk State University
Vol. 63, No. 4, pp. 519–542, 2022 *DOI:10.2113/RGG20214410* *Geologiya i Geofizika*

Sulfide PGE–Cu–Ni and Low-Sulfide Pt–Pd Ores of the Monchegorsk Ore District (Arctic Western Sector): Geology, Mineralogy, Geochemistry, and Genesis

V.V. Chashchin[a, ✉], V.N. Ivanchenko[b]

[a]*Geological Institute of the Kola Science Center, Russian Academy of Sciences, ul. Fersmana 14, Apatity, 184209, Russia*

[b]*AO Rosgeologiya, ul. Odoevskogo 24, St. Petersburg, 199155, Russia*

Received 2 August 2021; accepted 30 November 2021

Abstract—During the recent exploration of the Monchegorsk ore district (MOD) in the Arctic western sector, the platinum potential of known Cu–Ni deposits (Nittis-Kumuzhya-Travyanaya (NKT), Nyud, Ore Horizon 330 (OH330), and Terrasa) has been assessed, and new sulfide PGE–Cu–Ni deposits (Western Nittis) and manifestations (Moroshkovoe Ozero, Poaz, and Arvarench), and low-sulfide Pt–Pd deposits (Loipishnyun, Southern Sopcha, and Vuruchuaivench) have been discovered. All of them are confined to Paleoproterozoic (ca. 2.5 Ga) layered intrusions (the Monchegorsk pluton (Monchepluton) and the Monchetundra massif) and are divided into two types according to their structural position: basal, located in the marginal parts of intrusions, and reef-type (stratiform). All types of ores show Pd specialization. Platinum group minerals (PGM) have a limited composition in sulfide PGE–Cu–Ni ores and are represented by predominant Pt and Pd compounds with Bi and Te and subordinate PGE arsenides and sulfides. Low-sulfide Pt–Pd ores are characterized by a significant variety of PGM, with a predominance of PGE sulfides, bismuthide-tellurides, and arsenides. Sulfide PGE–Cu–Ni deposits and manifestations (Western Nittis, NKT, Nyud, Moroshkovoe Ozero, Poaz, and Arvarench) formed through the accumulation of base metal sulfides and PGE in immiscible sulfides and their subsequent segregation in commercial contents. The reef-type OH330 deposit and Terrasa manifestation resulted from the injection of additional portions of sulfur-saturated magma. The basal-type low-sulfide Pt–Pd deposits (Loipishnyun and Southern Sopcha) formed from residual melts enriched in ore components and fluids separated and crystallized during long-term ore-forming processes. The reef-type Vuruchuaivench deposit is the result of deep fractionation of the parental magma with the formation of a sulfide liquid enriched in Cu and PGE. Significant reserves and large predicted resources of sulfide PGE–Cu–Ni and low-sulfide Pt–Pd ores are a reliable mineral resource base for the development of the mining industry in the Kola region of the Arctic western sector.

Keywords: sulfide PGE–Cu–Ni and low-sulfide Pt–Pd ores; basal and reef types of deposits and manifestations; PGE geochemistry; platinum group minerals; Monchepluton; Monchetundra massif; Monchegorsk ore district

INTRODUCTION

The most significant reserves of platinum group metals are concentrated in the Russian Arctic zone. The largest ones are located in the Norilsk ore district, which provides 42% of the world palladium production (Gurskaya and Dodin, 2015). The PGE deposits in the Arctic western sector are also of great commercial importance. There are about thirty Paleoproterozoic layered intrusions in the northeast of the Fennoscandian Shield (Fig. 1). Some of them host large Cr, sulfide PGE–Cu–Ni, and low-sulfide Pt–Pd deposits and Ti and V occurrences. About ten of these intrusions are located in the Kola region, including several ore-bearing intrusions of the Monchegorsk and Fedorova–Pana ore districts.

The MOD ore potential is determined by PGE deposits spatially and genetically associated with the Monchepluton and the Monchetundra massif. The Monchepluton is the most mineral-productive as compared with other Paleoproterozoic layered intrusions of the Fennoscandian Shield. Therefore, the MOD can be considered one of the most important platinum-bearing areas in the Kola region. It is part of the Kola platinum-metal province (Mitrofanov et al., 1999), along with the Fedorova–Pana ore district, which is the second most important province in Russia after the Norilsk one.

Most of the Monchepluton sulfide Cu–Ni deposits have been known since the late 1930s. These deposits have been studied for a long time; as a result, rich vein and injection ores and poor disseminated ores were discovered in them. Vein ores were mined out in the middle 1970s, and injection and poor disseminated ores were regarded as unprofitable.

The platinum-metal potential of known MOD Cu–Ni deposits was estimated over the past 15 years, and search for new, including specific, types of mineral raw material, such as Cr and PGE ores, was performed. As a result, the platinum content of several known Cu–Ni deposits (NKT,

✉ Corresponding author.
E-mail address: chashchin@geoksc.apatity.ru (V.V. Chashchin)

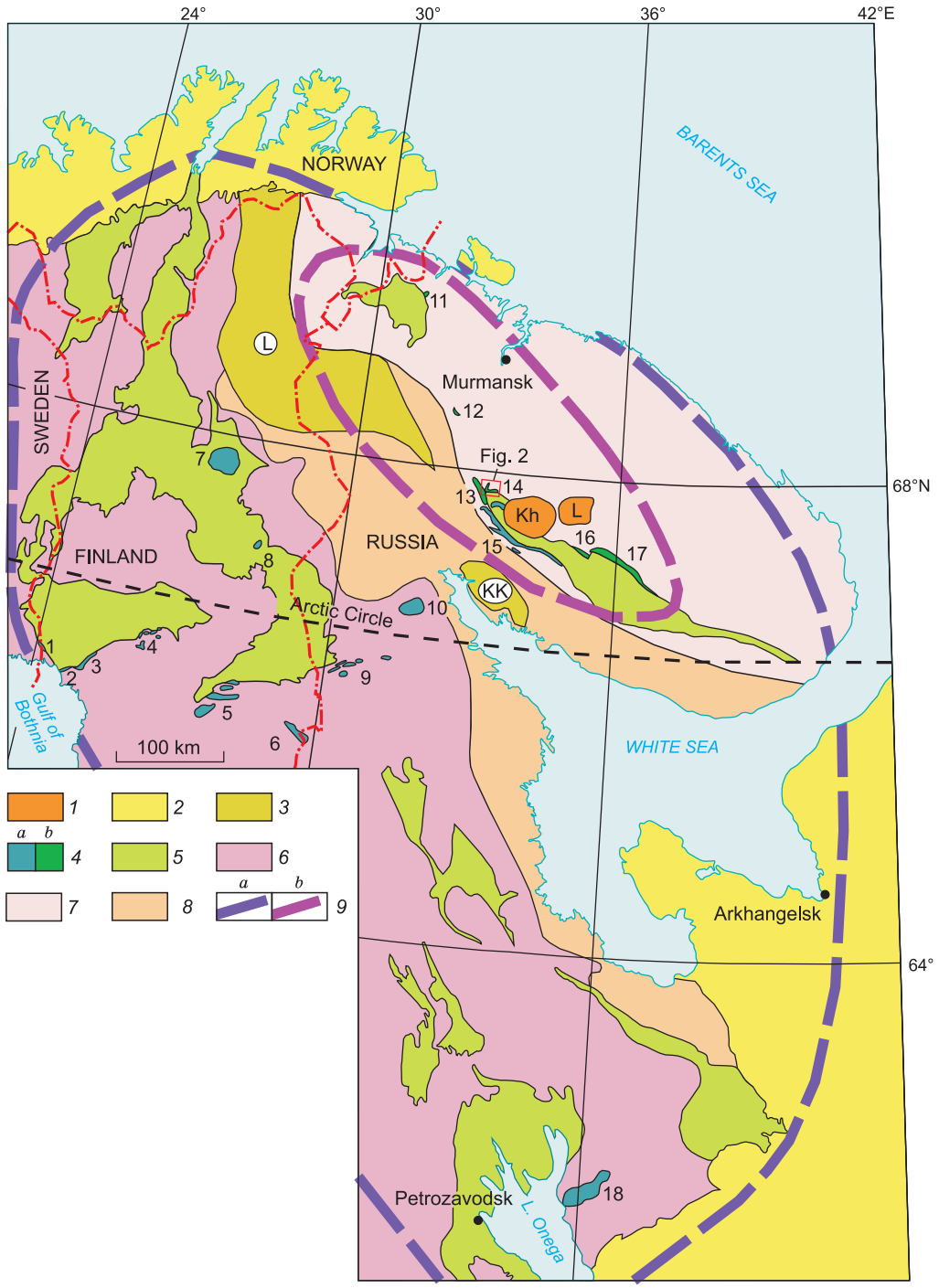

Fig. 1. Schematic map of the location of Paleoproterozoic layered intrusions of the northeastern Fennoscandian Shield of the European Arctic zone, modified from Gaál and Gorbatschev (1987), Alapieti et al. (1990), Sharkov and Bogatikov (1998), and Korovkin et al. (2003).
1, Paleozoic plutons of alkali nepheline syenites: Khibiny (Kh) and Lovozero (L); *2*, Neoproterozoic–Paleozoic sedimentary cover; *3*, Paleoproterozoic granulite belts: Lapland (L), Kandalaksha–Kolvitsa (KK); *4*, Paleoproterozoic layered intrusions: with an age of ca. 2.45 Ga (*a*), with an age of ca. 2.50 Ga (*b*); *5*, Paleoproterozoic rift volcanosedimentary structures; *6*, *7*, Archean provinces: *6*, Karelian, *7*, Kola; *8*, Belomorian Mobile Belt; *9*, outlines of mantle plumes: early (*a*) and late (*b*), after Smolkin et al. (2009). *1–18*, layered intrusions and complexes: 1, Tornio, 2, Kemi, 3, Penikat, 4, Portimo Complex, 5, Koillismaa Complex, 6, Näränkävaara, 7, Koitelainen, 8, Akanvaara, 9, Olanga Complex, 10, Kovdozero, 11, Mt. Generalskaya, 12, Ulitaozero, 13, Monchetundra, 14, Monchepluton, 15, Imandra Complex, 16, Fedorova Tundra, 17, Pana, 18, Burakovsko–Aganozero Complex.

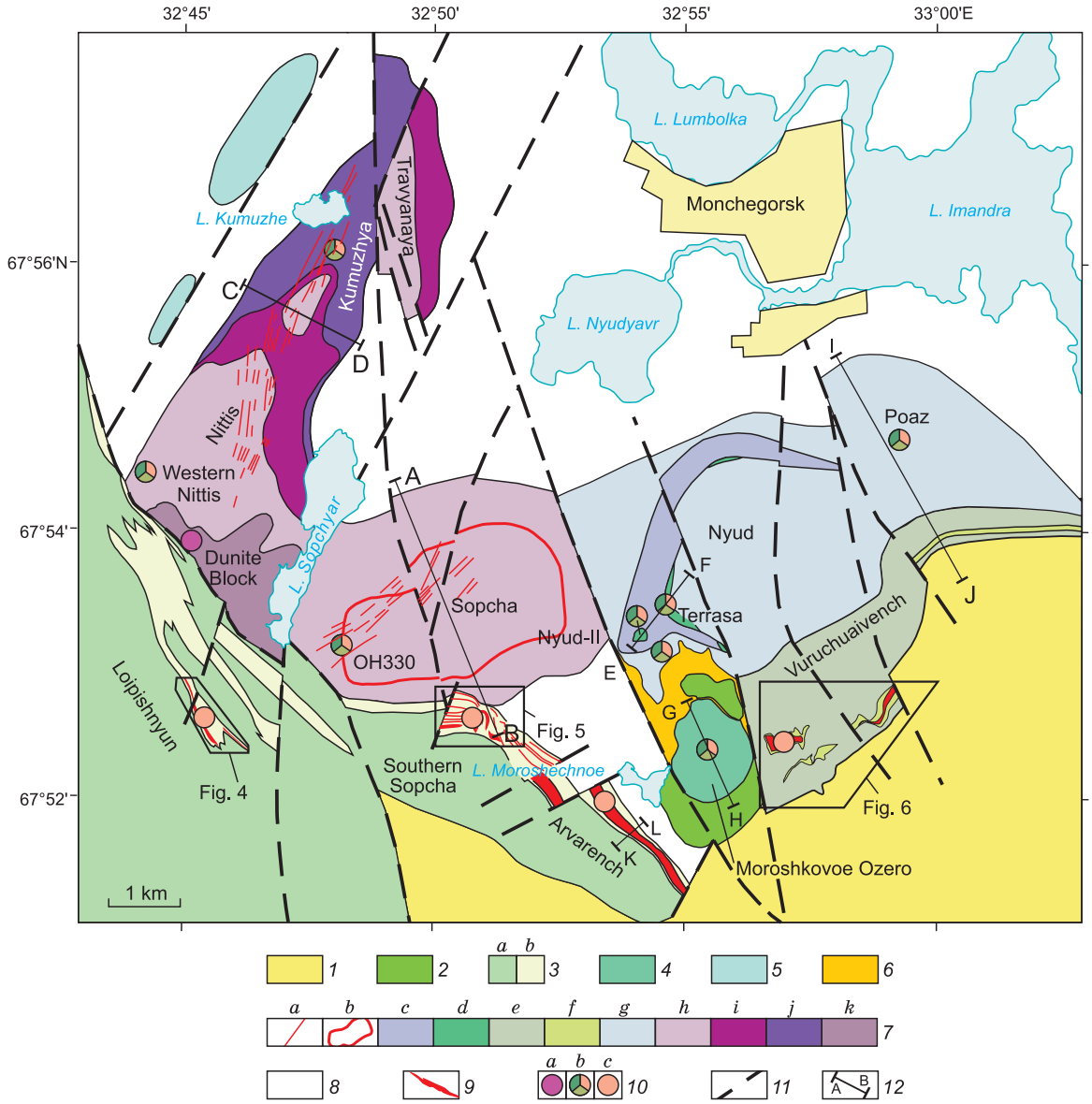

Fig. 2. Schematic geological map of the Monchegorsk ore district. *1*, Imandra–Varzuga rift structure: metavolcanic rock, quartzite, schist of varying composition, and conglomerate; *2*, metagabbro massif of the tenth anomaly; *3*, Monchetundra massif: upper zone – metagabbro, metagabbronorite, and anorthosite (*a*), lower zone – norite and orthopyroxenite (*b*); *4*, Moroshkovoe Ozero massif: norite and plagio-orthopyroxenite; *5*, Kirikha massif: gabbronorite; *6*, quartz diorite and trondhjemite; *7*, Monchepluton: sulfide veins (*a*), Ore Horizon 330 (*b*), olivine horizon (*c*), "critical" horizon (*d*), metagabbronorite (*e*), plagioclasite (*f*), norite (*g*), orthopyroxenite (*h*), alternating orthopyroxenite and harzburgite (*i*), harzburgite (*j*), dunite (*k*); *8*, Paleo-Neoarchean metamorphic and ultrametamorphic rocks of the Kola Province; *9*, zones of sulfide PGE mineralization; *10*, deposits and manifestations of: chrome ores (*a*), sulfide PGE–Cu–Ni ores (*b*), and low-sulfide Pt–Pd ores (*c*); *11*, faults; *12*, section lines.

OH330, Nyud, and Terrasa) was determined, and new PGE–Cu–Ni deposits and manifestations (Western Nittis, Moroshkovoe Ozero, Poaz, and Arvarench) were revealed. In addition, low-sulfide Pt–Pd deposits, such as Loipishnyun, Southern Sopcha, and Vuruchuaivench, were discovered (Fig. 2), which are new for the Kola region. At the same time, the large Sopcheozero Cr deposit in the Monchepluton was discovered and explored.

The goal of this paper is to consider the features of the geologic structure, mineral composition, and geochemical and genetic features of the MOD sulfide PGE–Cu–Ni and low-sulfide Pt–Pd deposits and manifestations, based on new prospecting and research data.

GEOLOGIC STRUCTURE OF THE NORTHEASTERN FENNOSCANDIAN SHIELD

The Monchegorsk ore district is located in the northeast of the Fennoscandian Shield comprising three large Archean geologic segments: the Kola and Karelian provinces and the Belomorian Mobile Belt (Fig. 1). The continental crust of the Kola and Karelian provinces is formed by tonalite–

trondhjemite–granodiorite (TTG) granite-gneiss with fragments of metasedimentary and metaigneous rocks and by supracrustal metavolcanic and metasedimentary rocks of Archean greenstone belts.

The Belomorian Mobile Belt lies between the Kola and Karelian Provinces (Fig. 1). It comprises the same structural and compositional assemblages as the neighboring provinces, but they experienced significant tectonic transformations in the Neoarchean and early and late Paleoproterozoic as a result of the collision of the Kola and Karelian provinces (Kozlov et al., 2006; Slabunov et al., 2021).

The Belomorian Mobile Belt includes the Lapland and Kandalaksha–Kolvitsa granulite belts (Fig. 1), which formed as individual tectonic structures in the late Paleoproterozoic (2.0–1.9 Ga) (Gaál and Gorbatschev, 1987; Balagansky et al., 2016). The age of their protolith formed by mafic and felsic metavolcanics (Kozlov et al., 1990) is still unclear. The granulite belt rocks were metamorphosed at high temperatures (800–1000 ºC) and pressures (9–12 kbar) and are thrust over the framing rocks in the southwest and southern directions (Mints et al., 1996; Balagansky et al., 2016).

The Paleoproterozoic magmatic events caused by the ascent of extensive mantle plume in this part of the Fennoscandian Shield led to the formation of numerous layered intrusions, volcanic rift structures, and dike swarms (Sharkov et al., 2000; Smolkin et al., 2009). The Fennoscandian layered intrusions are divided into two groups differing in age and relationship with volcanic rocks. The earlier layered intrusions (ca. 2.50 Ga) are overlapped with volcanic rocks with conglomerates at the base and exist only within the Kola Province. These are the Mt. Generalskaya and Ulitozero intrusions and the Monchegorsk and Fedorova–Pana complexes (Fig. 1) (Balashov et al., 1993; Amelin et al., 1995; Chashchin, 1999).

Later layered intrusions (ca. 2.45 Ga) breaking through the volcanic rocks of rift structures are more widespread. They are numerous in the Karelian Province (Tornio, Kemi, Penikat, Näränkävaara, Koitelainen, Akanvaara, and Kovdozero intrusions; Portimo, Koillismaa, Olanga, and Burakovsko–Aganozero complexes) (Alapieti et al., 1990; Alapieti and Lahtinen, 2002; Smolkin et al., 2009; Maier, 2015) and much less developed in the Kola Province (Imandra Complex) (Fig. 1). There are also numerous massifs of the so-called drusite complex, which formed in the Belomorian Mobile Belt at the same time and are similar in composition and age to the late layered intrusions (Sharkov et al., 2004; Krivolutskaya et al., 2010).

The layered intrusions of the both age groups differ in rock associations, the degree of differentiation, and ore contents. Some of them host Cr, Ni, Cu, PGE, Ti, and V deposits and manifestations, part of which are of commercial importance. In particular, the earlier ore-bearing layered intrusions are the most important component of the Monchegorsk and Fedorova–Pana ore districts.

GEOLOGY OF THE MONCHEGORSK ORE DISTRICT

The Monchepluton and the Monchetundra massif are major objects of the MOD (Fig. 2). The Monchepluton is of great scientific and practical interest, since it combines almost all types of deposits specific to layered intrusions, with atypical rich vein Cu–Ni ores. It is confined to the northwestern closure of the Imandra–Varzuga volcano-sedimentary rift structure and rests upon the Archean granitoid basement (Fig. 2). The Monchepluton is arcuate with an area of ca. 50 km^2 at the recent erosional-truncation level and consists of two branches of NE and E–W strikes (Gorbunov et al., 1985). The northeastern branch is more than 7 km long and ca. 2 km wide in the middle part and represents the NKT massif. The E–W branch is ca. 11 km long and ca. 3 km wide and comprises the Sopcha, Nyud, Poaz, and Vuruchuaivench massifs (Fig. 2). The Monchepluton can be divided into two parts ranked as subchambers in terms of the internal-structure peculiarities. The first subchamber includes the NKT and Sopcha massifs, up to 1000 and 1200 m thick, respectively, which are symmetrical troughs with flanks dipping at 20–45° to their axes. These massifs are formed mainly by ultramafic cumulates and have similar internal structures. Their sections are composed (from bottom to top) of ophitic gabbronorite (up to 100 m thick) at the basement, norite and orthopyroxenite in the marginal zone (10–100 m thick), dunite (100–700 m thick), developed only in the NKT massif (Dunite Block), harzburgite (100–200 m thick), interlaying harzburgite and orthopyroxenite (250–400 m thick), and orthopyroxenite (300–700 m). Ore horizon OH330 occurs in the middle part of the monotonous orthopyroxenite series of the Sopcha massif (Fig. 2), is 4–6 m in thickness, and is described in detail below. Probably, the parental magma of the ultramafic subchamber was similar in composition to the U-type high-Mg basalts of the Bushveld Complex (Barnes and Maier, 2002).

The second subchamber includes the Nyud, Poaz, and Vuruchuaivench massifs, up to 800, 400, and 700 m thick, respectively, and has a complex shape: trough-like in the north and gentle sheet-like in the south. These massifs are formed mainly by poorly differentiated mafic cumulates made up of norite and gabbronorite. The bottom of the vertical section of the Nyud massif is composed of up to 300 m thick melanonorite and plagio-orthopyroxenite, which are changed by up to 350 m thick mesocratic norite up the section. There is an olivine horizon between melanocratic and mesocratic norite in the western, northern, and southern parts of the massif, which is 6 km long and ca. 100 m thick, near-horizontal, and has a crescent shape (Fig. 2). It is formed by orthopyroxenite, plagio-orthopyroxenite, and melanonorite with a varying olivine content (up to 30 vol.% and occasionally higher), connected with each other by gradual transitions and steadily containing finely disseminated sulfides. The occurrence of the olivine horizon among

the massif rocks, which disturbs its normal stratigraphic sequence, indicates that it formed from magma of elevated basicity and sulfur saturation later than the Nyud rocks. The Poaz massif is composed of melanorite and plagiopyroxenite in the lower part (70–150 m thick) and mesocratic norite with subordinate gabbronorite interbeds in the upper part.

The Vuruchuaivench massif is located south of the Nyud and Poaz massifs (Fig. 2) and, according to drilling data, overlies them, being the uppermost part of the complete Monchepluton general section (Grokhovskaya et al., 2000; Mitrofanov and Smolkin, 2004; Rundkvist et al., 2014; Karykowski et al., 2018b). It extends northeastward for 6 km and is 0.5–2.0 km in width. The massif is characterized by a near-horizontal occurrence of rocks in the central part, which is changed by a southeastern dip at angles of up to 20–30° under the volcanogenic rocks of the Imandra–Varzuga rift structure. The bulk of the Vuruchuaivench massif is made up of monotonous meso- and melanocratic metagabbronorite, which is changed by a banded 200–240 m thick zone of mesocratic metagabbronorite with 5–50 m thick plagioclasite interbeds. The base of this zone includes a horizon of taxitic (from medium-grained to pegmatoid) metagabbronorite, with an interbed of ore-bearing plagioclasite in the upper part. The massif section is terminated with ca. 50 m thick leuco–mesocratic metagabbro and quartz metagabbronorite. The parental magma of the mafic subchamber was, most likely, similar in composition to the Bushveld tholeiitic basalt (Barnes and Maier, 2002).

Table 1 presents the age of some Monchepluton rocks estimated by zircon and baddeleyite U–Pb dating, which ranges from 2508 to 2484 Ma. According to the geochronological data, the marginal-zone quartz norite of the NKT massif is the earliest rock of the Monchepluton (2507 ± 9 Ma). The metagabbronorite and plagioclasite of the Vuruchuaivench massif have similar ages: 2504.2 ± 8.4 and 2507.9 ± 6.6 Ma (SIMS SHRIMP-II), respectively (Table 1), which contradict the geological data. The age of the Vuruchuaivench plagioclasite estimated by us earlier (2494 ± 4 Ma) is more likely (Table 1). The Dunite Block dunite and chrome ores are dated at ca. 2500 Ma, and the Nyud massif norite is somewhat younger, 2493 ± 7 Ma (Table 1), as well as the Poaz massif gabbronorite, 2496 ± 5 (oral communication by T.B. Bayanova). The ophitic gabbronorite at the NKT massif basement is a later intrusive phase; their U–Pb age (SIMS SHRIMP-II) is 2484.5 ± 7.9 Ma (Table 1).

The Monchetundra massif is an elongated oval in shape; its axis oriented northwestward plunges to the southeast. The massif is about 30 km in total length and 2–6 km in width. Its central part is about 2 km in vertical thickness according to deep structural drilling data, and its upper part and roof are eroded. The massif is trough-like in section, with the trachytoid and primary banding dipping toward its center. Its southeastern branch is named the Southern Sopcha massif (Fig. 2).

There are two zones in the internal structure of the Monchetundra massif: the lower norite–orthopyroxenite and up-

Table 1. The ages of the Monchepluton and Monchetundra massif rocks, determined by zircon (zrn) and baddeleyite (bdy) U–Pb dating

Massif	Rock	Age, Ma	Mineral	Reference
Monchepluton				
NKT	Ophite gabbronorite	2484.5 ± 7.9	zrn	(Chashchin and Savchenko, 2021a)
	Quartz norite of the marginal zone	2507 ± 9	zrn	(Mitrofanov and Smolkin, 2004)
Dunite Block	Dunite	2500 ± 10	zrn	(Chashchin and Bayanova, 2021)
	Chromitite	2500 ± 2	zrn	
Nyud	Gabbro-pegmatite	2504.4 ± 1.5	zrn	(Amelin et al., 1995)
	Gabbro-pegmatite	2500 ± 5	zrn, bdy	(Mitrofanov and Smolkin, 2004)
	Norite	2493 ± 7	zrn	(Balashov et al., 1993)
Nyud-II	Ore-bearing norite	2503 ± 8	zrn	(Chashchin et al., 2016)
	Orthopyroxenite	2506 ± 3	zrn	
Vuruchuaivench	Metagabbronorite	2497 ± 21	zrn, bdy	(Mitrofanov and Smolkin, 2004)
	Metagabbronorite	2498.2 ± 6.7	bdy	(Rundkvist et al., 2014)
	Metagabbronorite	2504.2 ± 8.4	zrn	
	Metaplagioclasite	2507.9 ± 6.6	zrn	
	Metagabbronorite	2504.3 ± 2.2	zrn	(Chashchin et al., 2016)
	Metaplagioclasite	2494 ± 4	zrn	
Monchetundra massif				
Loipishnyun	Orthopyroxenite	2496.3 ± 2.7	zrn	(Chashchin et al., 2020)
	Norite	2500 ± 2	zrn	
Southern Sopcha	Metagabbro	2478 ± 20	zrn	(Chashchin et al., 2016)
	Ore-bearing metanorite	2504 ± 1	zrn	

per leucogabbro–gabbronorite ones (Mitrofanov and Smolkin, 2004; Chashchin et al., 2020). The lower zone makes up about 20% of the massif volume. Its section is the most complete and well-preserved in the central (axial) part of the massif, reaching 450 m in thickness. The lower-zone basement is formed by orthopyroxenite and plagio-orthopyroxenite, which give way to meso- and melanocratic norite up the section. The lower-zone thickness gradually decreases to <50 m and is cut off by a fault on the southwestern flank. The lower zone has a more intricate geologic structure on the north-eastern flank. It is formed by 1–10 to 50–250 m thick blocks with irregular alternation of ortho- and plagio-orthopyroxenite with meso- and melanocratic norite, which are intruded by the upper-zone gabbroid (Chashchin et al., 2020).

The upper zone of the Monchetundra massif is ca. 80% of its volume and 500 to 1400 m in vertical thickness. It is made up of mesocratic medium-grained and, more seldom, coarse-grained, highly amphibolized leucocratic gabbronorite with a massive (in places, trachytoid) structure and of coarse-grained leucogabbro and, more seldom, anorthosite, usually occurring in the upper part of the zone. Sometimes, these rocks contain xenoliths of the lower-zone norite and orthopyroxenite. Note that in the 150–400 m wide Monchepluton zone adjacent to the Monchetundra massif, there are numerous transverse dikes of the upper-zone rocks of this massif (Chashchin et al., 2020).

The dunite and, more rarely, harzburgite occur within the lower and, less often, upper zones of the Monchetundra massif as numerous up to 50 m thick lenticular-sheet bodies serpentinized to a certain extent. They do not correlate with each other throughout the borehole section and occupy different positions in the lower-zone section. In general, these ultramafic rocks are, most likely, younger than the lower- and upper-zone rocks of the Monchetundra massif and are regarded as the result of oceanization of the continental-crust in the Kola Province (Chashchin and Savchenko, 2021b).

The orthopyroxenite and norite age in the Monchetundra massif lower zone is 2496.3 ± 2.7 and 2500 ± 2 Ma, respectively (Table 1). In general, this zone rocks are similar in petrogeochemical features and age to the same rocks of the Monchepluton (Chashchin et al., 2020).

The coarse-grained leucocratic metagabbro and metagabbronorite age in the upper zone of the Monchetundra massif varies from 2476 to 2453 Ma (Mitrofanov et al., 1993; Nerovich et al., 2009; Bayanova et al., 2010). Thus, the presented geological and geochronological data point to its multiphase formation.

Smaller mafic massifs are located south of the Nyud massif (Moroshkovoe Ozero) and northwest of the NKT massif (Kirikha). The Moroshkovoe Ozero massif is round, 1.4 × 1.1 km in size, and varies in vertical thickness from 75 m in the north to 350 m in the south. It is composed of predominant amphibolized norite with orthopyroxenite and subordinate gabbronorite interbeds and is intruded by metagabbro and diorite veins. We suppose that this massif was earlier the southern part of the Nyud massif but was detached from it later and displaced with an amplitude of ca. 700 m along NW striking faults.

The Kirikha massif comprises two intrusions. The larger one is lenticular and elongated in the northeastern direction parallel to the NKT massif. It is 2.5 km long and 650–700 m wide. The intrusion is composed mainly of mesocratic gabbronorite with olivine varieties at the basement and of quartz ferrogabbronorite in the roof. The age of olivine gabbronorite was estimated at 2502 ± 7 Ma, and the age of ferrogabbronorite, at 2500 ± 8 Ma (Chashchin et al., 2013).

METHODS

The Pt, Pd, Ni, Cu, and S contents were determined at ZAO Mekhanobr Inzhiniring Analit (St. Petersburg) and OAO Irgiredmet (Irkutsk) and used to calculate the average values, which are presented in Supplementary Material and shown below. The Pt and Pd contents were measured at ZAO Mekhanobr Inzhiniring Analit by the assay-atomic-absorption method on a Perkin Elmer 603 spectrophotometer (USA) with a preliminary assay concentration on a nickel matte. The Cu and Ni contents were determined by the atomic-absorption method (the same spectrophotometer), and the S content, by iodometric titration. The measurement errors depending on the content range were as follows (rel.%): Pt and Pd – 10–30; Cu and Ni – 10–50; and S – 1–14.

The Pt and Pd contents were determined at OAO Irgiredmet on an ICP ES IRIS Intrepid emission spectrometer (Thermo Elemental, USA) with a preliminary assay concentration of the metals on lead reguli. The Cu and Ni contents were measured by the atomic-absorption method on an ICAP 7400 DUO spectrometer (Thermo Fisher Scientific, USA). The S content was also determined by iodometric titration. The measurement errors depending on the content range were as follows (rel.%): Pt and Pd – 10–20, Cu and Ni – 10–40, and S – 1–14.

The contents of all PGE and Au in the ores of some deposits and manifestations were determined at OOO Institut Gipronikel (St. Petersburg) by ICP MS on an iCAP 6500 RQ mass spectrometer (Thermo Scientific, USA)) with a preliminary assay concentration on a nickel matte. The lower detection limits were as follows (ppm): Pd – 0.01, Pt – 0.005, and Au, Rh, Ru, Ir, and Os – 0.001. The determination errors were (rel.%) 30 (Pd), 40 (Pt), and 60 (Au, Rh, Ru, Ir, and Os).

The Cu and Ni contents were determined at the Institute of Geology and Geochemistry (Yekaterinburg) by ICP MS on a NexION 300S quadrupole mass spectrometer (Perkin Elmer, USA). The microwave decomposition of the samples with the acid mixture HCl + HNO_3 + HF was performed using a Berghof Speedwave MWS 3+ system. The accuracy of determination of these elements was controlled by analysis of certified basalt (BCR-2) and andesite (AGV-2) samples (USGS). The errors of determination of Cu and Ni contents were 24 rel.%.

GEOLOGY OF SULFIDE PGE–Cu–Ni AND LOW-SULFIDE Pt–Pd DEPOSITS AND MANIFESTATIONS

The Western Nittis and OH330 deposits and the NKT, Nyud, Poaz, Moroshkovoe Ozero, Arvarench, and Terrasa manifestations are of the sulfide PGE–Cu–Ni ore type, and the Loipishnyun, Southern Sopcha, and Vuruchuaivench deposits, of the low-sulfide Pt–Pd ones. All the deposits and manifestations are divided into two types according to their structural position: basal, localized within the underlying marginal parts of intrusions, and reef (stratiform) (Chashchin and Mitrofanov, 2014).

SULFIDE PGE–Cu–Ni DEPOSITS AND MANIFESTATIONS

The Western Nittis deposit is located at the southwestern margin of the Nittis massif (Fig. 2). The massif section here is made up of gabbronorite and norite in the marginal zone 10–50 m in thickness and of homogeneous orthopyroxenite in the rest part. The deposit comprises two structural types of sulfide ores: bottom deposit and massive-sulfide vein bodies. The bottom deposit is confined to the middle part of the marginal zone, traced for 800 m and oriented parallel to the contact with the host rocks. It consists of a series (one to three) of closely occurring sheet orebodies up to 16 m thick (on average, ca. 6 m). Ore mineralization occurs as disseminated pentlandite–chalcopyrite–pyrrhotite assemblage. According to O.V. Kazanov, 2016, the PGM are characterized by a predominance of sulfides (braggite) and a subordinate amount of arsenides (palladoarsenide) and tellurobismuthides (kotulskite and moncheite).

Vein and veinlet–disseminated postmagmatic PGE mineralization is localized in the zone of tectonized rocks in the upper part of the massif. There are two types of sulfide, essentially chalcopyrite veins. The first-type veins are of near-vertical orientation, impersistent in thickness, have uneven boundaries, and sometimes pass into sulfide schlieren. The second-type veins are orthogonal to the first-type ones, forming numerous thin veins and veinlets with sharp smooth boundaries (Kazanov et al., 2016). This type of ore is similar to the PGE–Cu veins of the axial part of the NKT massif in the type of mineralization and the proportion of PGM, Cu, and Ni. The main ore mineral in the veins is chalcopyrite, and the accessory minerals are millerite, pentlandite, and bornite. More than 20 PGE and Au minerals were found in these veins (Kazanov et al., 2016). Stannoarsenides, Pd-containing stannides (palarstanide and atokite), and Pt and Pd tellurobismuthides (kotulskite and moncheite) are predominant PGM. Pt–Fe alloys (isoferroplatinum) and arsenides (sperrylite and palladoarsenite) are less common; PGE sulfides (braggite, vysotskite, cooperite, and erlichmanite), plummbides (zvyagintsevite), tellurides (telargpalite), and sulfoarsenides (irarsite) are minor (Kazanov et al., 2016). The maximum contents of commercial elements in these ores are as follows: Ni – 0.32 wt.%, Cu – 2.05 wt.%, Pt – 6.5 ppm, and Pd – 98.8 ppm. The average contents of commercial elements in the deposit are presented in Table 2 and the metal reserves are shown in Table 3.

The OH330 deposit is localized in the orthopyroxenite of the upper part of the Sopcha massif (Fig. 3*a*). It is a sill-like sheet body 4–6 m in thickness (up to 13 m in some swells), traced by drilling for 3.3 km and up to 1.8 km in

Table 2. Average contents of metals and sulfur and geochemical parameters in the sulfide PGE–Cu–Ni deposits and manifestations and low-sulfide Pt–Pd deposits of the Monchegorsk ore district

Deposits and manifestations	Ni	Cu	S	Pt	Pd	Pt + Pd	Pd/Pt	Cu/Ni	Cu/Pd	(Pt + Pd)/S	(Ni + Cu)/(Pt + Pd)
	wt.%			ppm							
Sulfide PGE–Cu–Ni deposits and manifestations											
Western Nittis[1]	0.18	0.13	0.58	0.22	1.20	1.42	5.5	0.72	1083	2.45	2183
OH330[2]	0.46	0.23	0.62	0.24	0.93	1.17	3.9	0.50	2473	1.89	5897
NKT[3]	0.38	0.16	1.57	0.13	0.75	0.88	5.8	0.42	2133	0.56	6136
Nyud[3]	0.29	0.24	1.11	0.11	0.73	0.84	6.6	0.83	3288	0.76	6310
Moroshkovoe Ozero[3]	0.25	0.20	0.61	0.13	0.82	0.95	6.3	0.80	2439	1.56	4737
Poaz[4]	0.17	0.13	0.39	0.13	1.11	1.24	8.5	0.76	1171	3.18	2419
Arvarench[2]	0.08	0.25	0.42	0.34	1.18	1.52	3.5	3.13	2950	3.62	2171
Terrasa[3]											
upper reef	0.19	0.13	0.76	0.28	1.04	1.32	3.7	0.67	1241	1.74	2444
lower reef	0.19	0.17	0.81	0.09	0.67	0.76	7.0	0.90	2597	0.94	4794
Low-sulfide Pt–Pd deposits											
Loipishnyun[1]	0.08	0.09	0.23	0.47	0.79	1.26	1.7	1.13	1139	5.48	1349
Southern Sopcha[2]	0.11	0.10	0.27	0.33	1.09	1.42	3.3	0.91	917	5.26	1479
Vuruchuaivench[2]	0.18	0.25	0.39	0.35	2.71	3.06	7.7	1.39	923	7.85	1405

Note. The average contents of metals and sulfur and the reserves and predicted resources of metals in Tables 2 and 3 are given after [1]O.V. Kazanov, 2016, [2]V.N. Ivanchenko, 2009, [3]V.N. Ivanchenko, 2017, and [4]V.N. Ivanchenko, 2020.

Table 3. The metal reserves and resources in the sulfide PGE–Cu–Ni deposits and manifestations and low-sulfide Pt–Pd deposits of the Monchegorsk ore district

Deposits and manifestations	Ni	Cu	Pt	Pd	Pt + Pd
	thousand tons		tons		
Sulfide PGE–Cu–Ni deposits and manifestations					
Westhern Nittis[1]	12	9	2	8	10
OH330[2]	218	109	11	44	55
NKT[3]	298	229	19	55	74
Nyud[3]	220	188	6	27	33
Moroshkovoe Ozero[3]	208	172	8	37	45
Poaz[4]	649	443	41	342	383
Arvarench[2]	79	246	33	116	149
Terrasa[3]					
upper reef	70	46	10	37	47
lower reef	95	88	4	28	32
Low-sulfide Pt–Pd deposits					
Loipishnyun[1]	23	24	13	23	36
Southern Sopcha[2]	50	46	15	49	64
Vuruchuaivench[2]	23	31	4	34	38

width along the entire perimeter of the Sopcha massif, and gently dipping (5–15º) to the axial part of the massif.

The thickest and most complete section of the OH330 deposit was stripped in the outcrops in its western part. Its general composition is as follows (from bottom to top): olivine orthopyroxenite, dunite, harzburgite, orthopyroxenite with different grain sizes, and olivine orthopyroxenite similar to those at the section basement. The deposit section is commonly reduced in the eastern direction because of the significant decrease (up to the absence) in the amounts of dunite and harzburgite; on the eastern flank it is made up only of orthopyroxenite.

The zircon age (SIMS SHRIMP-II) of coarse-grained orthopyroxenite from the OH330 deposit is 2492.5 ± 4.1 Ma (oral communication by S.A. Sergeev); $\varepsilon_{Nd} = -6.0 \pm 0.6$, according to Sm–Nd isotope data for harzburgite (Chashchin et al., 2016). These data point to the later formation of the OH330 deposit as compared with the Sopcha massif host orthopyroxenite. Additionally, the OH330 rocks formed from a mantle source that had undergone a more significant crustal contamination than the mantle source of the Sopcha orthopyroxenite, whose ε_{Nd} value varies from +1.2 to –2.3 (Mitrofanov and Smolkin, 2004).

The OH330 rocks contain sulfide (chalcopyrite–pentlandite–pyrrhotite) dissemination in the amount from occasional grains to 2–3 vol.% in coarse-grained orthopyroxenite and in the upper part of harzburgite interbed. Millerite, bornite, pyrite, and oxide ore minerals (chromite and magnetite) are subordinate (Neradovsky et al., 2002; Mitrofanov and Smolkin, 2004). Platinum group minerals are predominantly Pt–Fe alloys (isoferroplatinum) and, more seldom, arsenides (sperrylite), tellurobismuthides (kotulskite and moncheite), tellurides (sopcheite and merenskyite), and bismuthide–tellurides (michenerite) in harzburgite. On the contrary, tellurobismuthides (moncheite and kotulskite), tellurides (keithconnite), and bismuthide–tellurides (michenerite) are predominant, and arsenides (sperrylite), unnamed Pt–Fe alloys, and sulfides (cooperite) are subordinate in coarse-grained orthopyroxenite (oral communication by S.V. Petrov). The average contents of commercial elements in the deposit ore are presented in Table 2, and the metal reserves are shown in Table 3. A specific feature of the deposit is the maximum average Ni content in the ore among all the studied MOD deposits and manifestations (Ni = 0.46 wt.%, Table 2). Grokhovskaya et al. (2003) reported the highest PGE contents (up to 8.0 ppm) in the roof of coarse-grained orthopyroxenite interbed, but these data were not confirmed by later studies. The concentrate obtained during technological ore processing tests showed the following recovery of commercial elements: Ni – 74%, Cu – 86%, Pt – 68%, and Pd – 80%.

The NKT manifestation is localized in the rocks of the marginal zone of the Kumuzhya massif (Fig. 3*b*): taxitic, medium- and coarse-grained olivine- and olivine-free plagio-orthopyroxenite and melanonorite, and, more seldom, quartz norite. It occurs both near the massif basement and at a distance of 8–30 m above it (a bottom deposit). Sometimes, mineralization is absent from orthopyroxenite but occurs in overlying harzburgite, 10–15 m above the massif basement, and also in ophitic gabbronorite located 30 m below the basement. The ore zone comprises one or two orebodies and is generally sheet-like and conformal to the massif basement roughness. It is 900 m wide in the northern part of the massif and 1200 m wide in the central part. The zone has an intricate structure because of the impersistent thickness (from 2–5 to 60–80 m), pinches and swells, and the uneven distribution of sulfide mineralization. Nested–disseminated sulfides (chalcopyrite, pentlandite, and pyrrhotite) amount to 1–5 vol.%. Their grains vary in size from 1.0–1.5 mm to 2.0 cm and are usually localized in silicate interstices, and the largest nests often contain orthopyroxene and olivine inclusions. The PGM are tellurobismuthides (kotulskite), bismuthide-tellurides (moncheite and michenerite), tellurides (merenskyite), and bismuthides (frudite) according to the data obtained by V.N. Ivanchenko in 2017. The average contents of commercial elements found in the ores are presented in Table 2, and their predicted resources are shown in Table 3. The maximum contents of these elements are as follows: Ni – 1.82 wt.%, Cu – 0.46 wt.%, and (Pt + Pd) – 4.5 ppm. Technological ore processing tests showed a high quality of the concentrate with the following recovery of commercial elements: Ni – 88%, Cu – 89%, Pt – 66%, and Pd – 87%.

The Nyud manifestation is localized in the south of the Nyud massif, at the site bounded by NW striking faults. Its ore zone is 2.8 km long and up to 1.3 km wide, confined to the lower part of the massif section, composed of melanonorite and plagio-orthopyroxenite, and consists of one or two

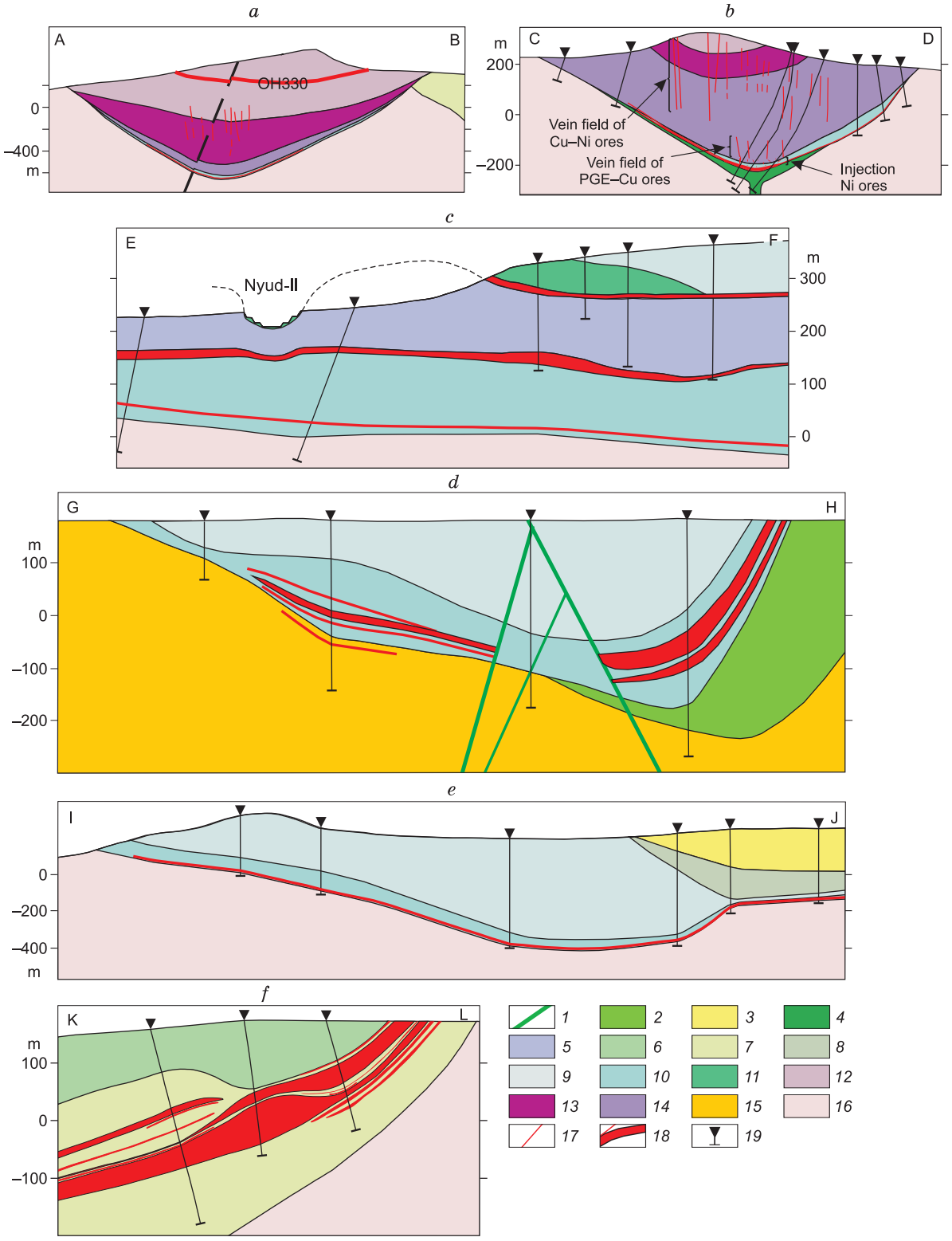

Fig. 3. Schematic geologic sections along the lines whose position is shown in Fig. 2: *a*, A–B (Sopcha massif), *b,* C–D (NKT massif), *c*, E–F (Nyud massif), *d*, G–H (Moroshkovoe Ozero massif), *e*, I–J (Poaz massif), *f*, K–L (Arvarench massif). *1–16*, rocks: *1*, metadolerite dikes, *2*, quartz metagabbro, *3*, metavolcanic rocks, *4*, ophite gabbronorite, *5*, olivine horizon, *6*, leucocratic metagabbro and metagabbronorite, *7*, norite and orthopyroxenite, *8*, metagabbronorite with metaplagioclasite interbeds, *9*, mesocratic norite, *10*, melanonorite and plagio-orthopyroxenite, *11*, "critical" horizon, *12*, orthopyroxenite, *13*, alternating harzburgite and orthopyroxenite, *14*, harzburgite, *15*, quartz diorite and trondhjemite, *16*, quartz gneiss-diorite, *17*, sulfide veins, *18*, ore zones and sulfide mineralization bodies, *19*, boreholes.

orebodies. The lower 4–12 m thick orebody occurs near the massif basement or slightly above it. The upper 3–7 m thick orebody lies 10–30 m above the basement (Fig. 3*c*).

Sulfide mineralization is mostly disseminated (1–3 vol.% sulfides) and nested–disseminated (3–5 vol.% sulfides). The veinlets of massive sulfides up to 15 cm thick and zones of veinlet sulfide mineralization 0.5 m thick (30–40 vol.% sulfides) are less common. The average contents of commercial elements are presented in Table 2, and their predicted resources are shown in Table 3. The maximum contents of these elements in zones with high-grade sulfide mineralization are as follows: Ni – 3.25 wt.%, Cu – 6.0 wt.%, Pt – 0.19 ppm, and Pd – 2.79 ppm.

The Moroshkovoe Ozero manifestation is localized in the lower part of the Moroshkovoe Ozero massif, mainly in plagio-orthopyroxenite and, less, in norite and in the zone of their alternation. The manifestation occupies a significant vertical range (40–160 m), beginning at depths of 130 and 215 m and ending near the massif basement (Fig. 3*d*). There are two to six orebodies 1.3–46 m in thickness, forming an ore zone with a total thickness of 14–77 m (on average, ca. 50 m). Two types of PGE distribution throughout the zone section are observed: (1) the minimum PGE content in the lower and upper orebodies, high contents in the middle orebodies, and the maximum content in the orebody third from the bottom; (2) the maximum PGE, Ni, and Cu contents in the lower orebody and low PGE and S contents in three upper orebodies. Sometimes Cu-enriched (Cu/Ni = 4.2) sulfide mineralization with Pt + Pd = 1.37 ppm, ca. 4 m in thickness, occurs in the underlying diorite at a distance of up to 10 m from the massif basement.

The ore mineralization is fine sulfide dissemination (1–2 vol.% sulfides), nested–disseminated sulfides (up to 3–5 vol.%), and is also present in schlieren, fine stringers, and 10–30 cm thick interbeds of high-grade brecciform ores with 10–40 vol.% sulfides. The maximum contents of commercial elements in sulfide-rich ores are as follows: Ni – 5.2 wt.%, Cu – 8.8 wt.%, Pt – 0.9 ppm, and Pd – 8.2 ppm. The average contents of these elements are presented in Table 2, and their predicted resources are shown in Table 3. Of special interest is the sulfide mineralization of essentially chalcopyrite composition found in coarse-grained metagabbro south of the Moroshkovoe Ozero massif. The orebody here reaches 22.5 m in thickness and is characterized by the following average contents of commercial elements: Ni – 0.09 wt.%, Cu – 0.70 wt.%, Pt – 0.13 ppm, and Pt – 0.89 ppm.

The Poaz manifestation is localized mainly in the melanonorite and plagio-orthopyroxenite of the lower part of the Poaz massif (Fig. 3*e*). The ore zone 10 to 50 m in thickness is traced for 2.4 km in the E–W direction and for 2.7 km in the N–S direction and comprises one to three orebodies. The lower orebody is confined mostly to the massif basement or, less often, occurs 10–15 m above it. The two upper orebodies occur 20–50 m above the basement. The orebodies have a varying thickness, 2–30 m (on average, ca. 6 m), with pinches and swells.

Sulfide mineralization in the ore has a pyrite–pentlandite–chalcopyrite–pyrrhotite composition and is found as fine dissemination or, more seldom, nests (1–5 vol.%). The PGM here are dominated by tellurobismuthides (kotulskite and moncheite), tellurides (merenskeyite), bismuthides (froodite and sobolevskite), bismuthide–tellurides (michenerite), and bismuthide–antimonides (insizwaite), Pd stannides (paolovite and atokite) and arsenides (sperrylite and palladoarsenite) are subordinate, and Pt–Fe alloys (isoferroplatinum) and Pd plumbites (zvyagintsevite) are minor, according to the data obtained by V.N. Ivchenchenko in 2020. The average contents of commercial elements are presented in Table 2, and their predicted resources are shown in Table 3. showed the following possible recovery of commercial elements: Technological tests showed a high quality of the concentrate with the following recovery of commercial elements: Ni – 69%, Cu – 89%, Pt – 72%, and Pd – 84%.

The Arvarench manifestation is localized on the southeastern extension of the Southern Sopcha deposit (Fig. 2) and is confined to the norite and plagio-orthopyroxenite of the lower zone of the Southern Sopcha massif, intruded by the coarse-grained gabbro and gabbronorite veins of the upper zone. It comprises several proximal 6–40 m thick orebodies with sulfide dissemination, united into a sheet-like ore zone ca. 70 m in total thickness (Fig. 3*f*). The zone has an intricate internal structure and morphology because of alternating ore and ore-free sites, pinches, and swells. It is of NW strike (310–320º) and SW dip (15–20º), 3 km long, and is traced for 280–500 m along the dip. The average contents of commercial elements are presented in Table 2, and their predicted resources are shown in Table 3. A specific feature of the manifestation is significant domination of Cu over Ni (Cu/Ni = 3.13) and the maximum average PGE content (Pt + Pd = 1.52 ppm, Table 2) among the studied MOD PGE–Cu–Ni deposits and manifestations.

The Terrasa manifestation is localized in the west of the Nyud massif (Fig. 2). It is spatially associated with a 100–200 m thick olivine horizon and comprises two reef orebodies. There is the small Nyud-II sulfide PGE–Cu–Ni deposit within its area, abandoned in the 1970s (Fig. 3*c*) (Chashchin et al., 2021).

The upper reef is confined to the olivine orthopyroxenite roof at its contact with the gabbronorite of the 70–80 m thick "critical" horizon marked by a thin interbed of fine-grained plagioclase–pyroxene hornfels. This horizon is overlain by the Nyud mesocratic norite (Fig. 3*c*). The upper reef is a gently sloping bed ca. 600 m long and ca. 10 m in average thickness, which gradually wedges out to the east. It is composed mostly of clinopyroxene- and plagioclase-containing olivine orthopyroxenite.

The lower reef is confined to the exocontact of the olivine horizon and occurs among the melanocratic poikilitic norite of the lower zone of the Nyud massif (Fig. 3*c*). It is ca. 1.5 km in length and varies in thickness, up to 20 m in the western part of the reef, which gradually decreases eastward, averaging ca. 10 m. Sulfide mineralization is present

in both reefs as fine or medium-sized dissemination and, less often, as 1–5 cm nests and amounts to 1–3 vol.%. The main ore minerals are pyrrhotite, pentlandite, and chalcopyrite, and the accessory minerals are pyrite, titanomagnetite, ilmenite, and chromite. The PGM compositions in the two reefs are similar to each other: tellurides (merenskyite), tellurobismuthides (moncheite and kotulskite), bismuthide-tellurides (michenerite), and bismuthides (sobolevskite) (oral communications by S.V. Petrov and E.E. Savchenko). The average contents of commercial elements in each reef are presented in Table 2, and their predicted resources are shown in Table 3.

LOW-SULFIDE Pt–Pd DEPOSITS

A distinctive feature of low-sulfide Pt–Pd deposits is enrichment in PGE relative to sulfide mass and subordinate Ni and Cu contents (Sluzhenikin et al., 1994, 2020; Dodin et al., 2000; Naldrett, 2003, 2010; Green and Peck, 2005; Sharkov, 2006; Sluzhenikin et al., 2020). Low-sulfide Pt–Pd deposits belong to the most important geologic and commercial type, like the leading world PGE deposits, such as the Merensky Reef of the Bushweld Complex (South Africa), J–M Reef of the Stillwater Complex (USA), and the Main Sulfide Zone of the Great Dyke (Zimbabwe), which are the main suppliers of PGE to the world market.

The Loipishnyun deposit is located in the northeast of the Monchetundra massif, near the zone of its contact with the NKT massif of the Monchepluton (Fig. 2). The deposit occurs mostly in the hanging wall of the lower norite–orthopyroxenite zone of the massif, near the contact with the host gabbroid (Fig. 4). It includes two ore zones. Ore zone 1 is 10–15 to 120 m thick and is traced for ca. 1.5 km in the northwestern direction. It has a complex structure because of alternating 90–120 m thick and up to 100 m long swells, 15 m thick pinches, and wedging-out of ore (Fig. 4). The thickness of the ore zone decreases along the dip within the first 100–150 m, and the orebodies become split into thin interbeds and lenses, which is accompanied by a decrease in PGE contents. The ore zone comprises 2–9 lenticular-sheet orebodies 0.5–25.0 m in thickness. The orebodies are often intruded by ultramafic rocks and dikes of coarse-grained gabbroid and metadolerite and are also displaced along tectonic zones (Fig. 4) (Chachshin et al., 2018).

Ore zone 2 is 5–35 m in thickness; it is traced for 550 m and is cut by N–S striking fault on the northwestern flank (Fig. 4). It is characterized by persistent occurrence but uneven distribution of sulfide mineralization, expressed as alternation of 2–10 m thick low-mineralization beds and 3–15 m thick ordinary-mineralization ones. There are also lenses of high-grade ores and 0.5–2.5 m thick ore-free interbeds (Chashchin et al., 2018).

Sulfide mineralization is present mostly as fine dissemination (ca. 1–2 vol.%) or, in places, as dense dissemination (3–5 vol.%) and, seldom, as veinlet–nest aggregates of pyrrhotite, pentlandite, and chalcopyrite. In addition, later sulfides are present: pyrite, bornite, chalcocite, cubanite, and makinavite; galena and sphalerite are minor. The oxide minerals are magnetite, ilmenite, and rutile (Chashchin et al., 2018).

Forty-five PGM were found in the ore, with sulfides (cooperite, braggite, and vysotskite), tellurobismuthides (moncheite and kotulskite), tellurides (keithconnite, telargpalite, and telluropalladinite), Pt–Fe alloys (isoferroplatinum), and arsenides (sperrylite, palladoarsenide, stillwaterite, and atheneite) being predominant and PGE–Cu minerals (skaergardite and hongshiite), native palladium, stannides (stannopalladinite), and plumbides (zvyagintsevite) being subordinate (Chashchin et al., 2018). The average contents of commercial elements in the ore are presented in Table 2, and their reserves are shown in Table 3.

The Southern Sopcha deposit is located in the northeast of the Southern Sopcha massif, in the zone adjacent to the Sopcha massif of the Monchepluton (Fig. 2). It is confined to the alternating taxitic norite and orthopyroxenite of the 150–200 m thick lower zone of the massif, being developed mainly in the norite. The deposit ore zone is ca. 1 km long and 100–500 m wide and comprises about 20 sheet and lenticular–flat orebodies traced for 100–500 m along the dip and varying in thickness from 1 to 78 m (ca. 5–30 m) (Fig. 5). The orebodies are cut by a NE striking fault in the west of the deposit. They are crushed to synform folds with a limb span of ca. 300 m and a vertical amplitude of ca. 90 m at the center.

Sulfide mineralization is found as dissemination, nests, and thin stringers of millerite–bornite–pyrrhotite–chalcopyrite composition (2–5 vol.%) in the norite. It is present as fine dissemination of pentlandite–pyrrhotite–chalcopyrite composition (1–2 vol.%) in the orthopyroxenite. The PGM composition is characterized by species diversity with a wide development of arsenides (sperrylite, palladoarsenide, stillwaterite, arsenopalladinite, and isomertieite) and tellurobismuthides (moncheite and kotulskite). Sulfides (cooperite and braggite), stannides (atokite and rustenburgite), and intermetallic compounds are less common (Grokhovskaya et al., 2012). The average contents of commercial elements in the ore are presented in Table 2, and their reserves are shown in Table 3.

The Vuruchuaivench deposit is clearly stratiform and is confined to the horizon of saussuritized plagioclasite. The deposit ore zone is about 2 km long and includes several sheet-like and lenticular orebodies 3–6 m thick and up to 300–500 m long, subconcordant to the plagioclasite boundaries (Grokhovskaya et al., 2000). Some orebodies are complicated by ca. 20 m thick swells, which are accompanied by a series of 2–3 m thick lenticular tongues. The ore zone is of near-horizontal occurrence (60–240) × 600 m and (30–70) × 650 m in size (Fig. 6) in the west and in the east of the deposit, respectively. It is traced for 1200 m along the dip, tending to flattening.

The deposit PGE mineralization is intimately associated with sulfide dissemination, which is unevenly distributed:

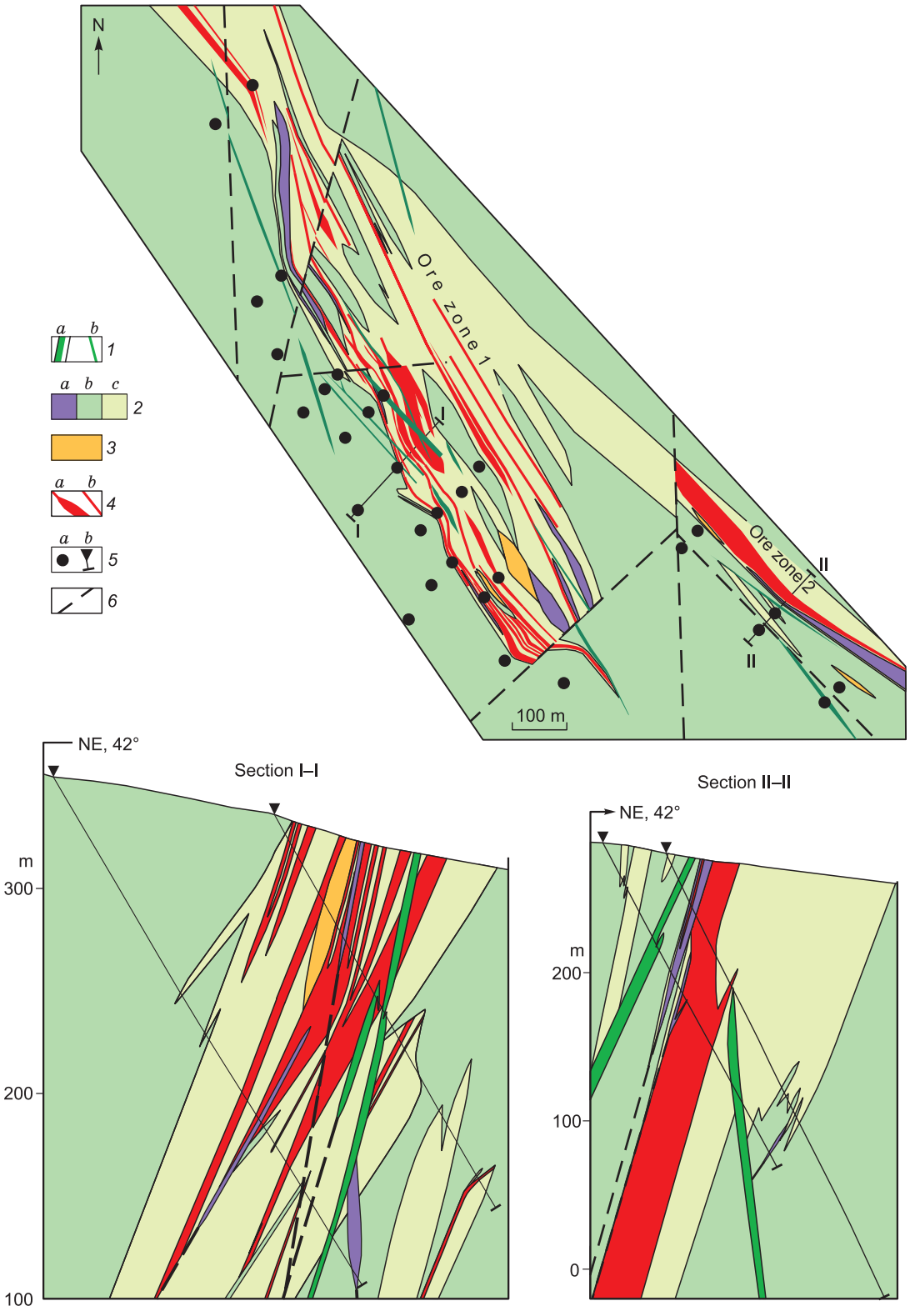

Fig. 4. Scheme of the geologic structure of the Loipishnyun low-sulfide PGE deposit with sections I–I and II–II, after Chashchin et al. (2018). *1*, metadolerite dikes (*a*), the same out of scale (*b*); *2*, Monchetundra massif: dunite and harzburgite (*a*), metagabbronorite and medium- to coarse-grained leucocratic metagabbro (*b*), orthopyroxenite and melanonorite (*c*); *3*, staurolite–garnet–biotite gneiss; *4*, low-sulfide PGE ore (*a*), the same out of scale (*b*); *5*, boreholes (*a*), the same in the sections (*b*); *6*, faults.

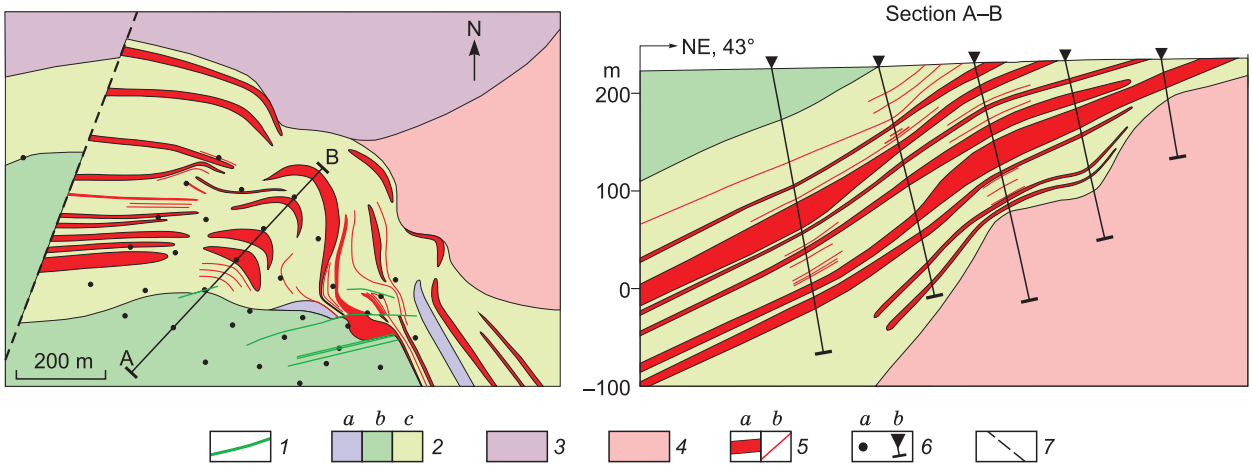

Fig. 5. Scheme of the geologic structure of the Southern Sopcha low-sulfide PGE deposit and A–B section, after data obtained by Ivanchenko in 2009. *1*, metadolerite dikes; *2*, Southern Sopcha massif: metaperidotite (talc–chlorite–amphibole schist) (*a*), metagabbro and metagabbronorite (*b*), orthopyroxenite and melanonorite (*c*); *3*, Sopcha massif: orthopyroxenite; *4*, diorite; *5*, low-sulfide PGE ore (*a*), the same out of scale (*b*); *6*, boreholes (*a*), the same in the section (*b*); *7*, faults.

from single nests 1–2 mm in size (ca. 1 vol.%) to nested dissemination measuring 1–5 mm (2–3 vol.%) and, more seldom, nest–schlieren accumulations (5–10 vol.%). The sulfides are predominant chalcopyrite (40–90 vol.%) and millerite (10–50 vol.%) and subordinate pyrrhotite, pentlandite, covellite, chalcocite, and pyrite. There are also sulfoarsenides of nickel (gersdorfite) and cobalt (cobaltite), sphalerite, and galena. The diversity of ore parageneses reflects the postmagmatic stage of ore formation (Grokhovskaya et al., 2000). The PGM are represented by tellurobismuthides (kotulskite), tellurides (merenskyite), bismuthide–tellurides (michenerite), bismuthides (sobolevskite), arsenides (sperrylite, guanglinite, and mayakite), and sulfoarsenides (hollingworthite, irarsite, and platarsite) (Grokhovskaya et al., 2000). The Vuruchuaivench deposit is characterized by the maximum average Pt + Pd contents among all the studied MOD PGE deposits and manifestations (Table 2). The average contents of commercial elements in the ore are presented in Table 2, and their reserves are shown in Table 3. Technological ore processing tests showed a high quality of the concentrate with the following recovery of commercial elements: Ni – 78%, Cu – 90%, Pt – 65%, and Pd – 88%.

Figure 7 presents a generalized localization model of PGE ores of different types in the MOD intrusions. It demonstrates a regular localization of ores as a result of the ore-magmatic evolution of ultramafic and mafic subchambers. It is remarkable that each of the subchambers has basal deposits and manifestations at the basement and reef ones in the upper part. The position of these PGE deposits is similar to that of PGE deposits in the layered Portimo Complex, Finland (Iljina et al., 2015) but differs from the position of basal and reef deposits of the Fedorova–Pana ore district, which are confined to different massifs: Fedorova Tundra and West Pana, respectively (Groshev et al., 2019).

GEOCHEMISTRY OF CHALCOPHILE AND SIDEROPHILE ELEMENTS

The existence of two types of PGE deposits in the MOD makes it necessary to consider numerical criteria for their difference from each other. One of them is the relative PGE concentration, which is calculated as the ΣPGE (ppm)/S (wt.%) value and is ≥4 for low-sulfide Pt–Pd deposits, according to Sluzhenikin et al. (1994), thus reflecting the enrichment in PGE relative to sulfides. We supplemented this index with the (Ni + Cu)/(Pt + Pd) value, which is <2000 for low-sulfide Pt–Pd ores and >2000 for sulfide PGE–Cu–Ni ores. The joint use of the two values permits a reliable distinguishing between the sulfide and low-sulfide types of PGE deposits, as shown in Fig. 8, where all types of MOD PGE ores are divided into three clusters. The first cluster comprises low-sulfide Pt–Pd deposits (Loipishnyun, Southern Sopcha, and Vuruchuaivench) and reef PGE mineralization of the Penikat intrusion, Finland (Alapieti and Lahtinen, 2002). The second cluster unites sulfide PGE–Cu–Ni deposits and manifestations (NKT, OH330, Moroshkovoe Ozero, Nyud, and the lower Terrasa reef). The third cluster is transitional between the above two, and its members (Western Nittis, Poaz, Arvarench, and the upper Terrasa reef) have features of both low-sulfide and sulfide deposits (Fig. 8).

The weighted average contents of chalcophile and siderophile elements in the orebodies of sulfide PGE–Cu–Ni and low-sulfide Pt–Pd deposits and manifestations with (Pt + Pd) ≥ 0.5 ppm are given in Supplementary, and their ratios are shown in Figs. 9 and 10. Sulfide PGE–Cu–Ni deposits and manifestations are characterized by a significant positive correlation between Ni and S, which is the highest in the Moroshkovoe Ozero manifestation, and most of the figurative points of Ni and S contents form a single trend (Fig. 9*a*). The exception is the OH330 deposit, the figurative

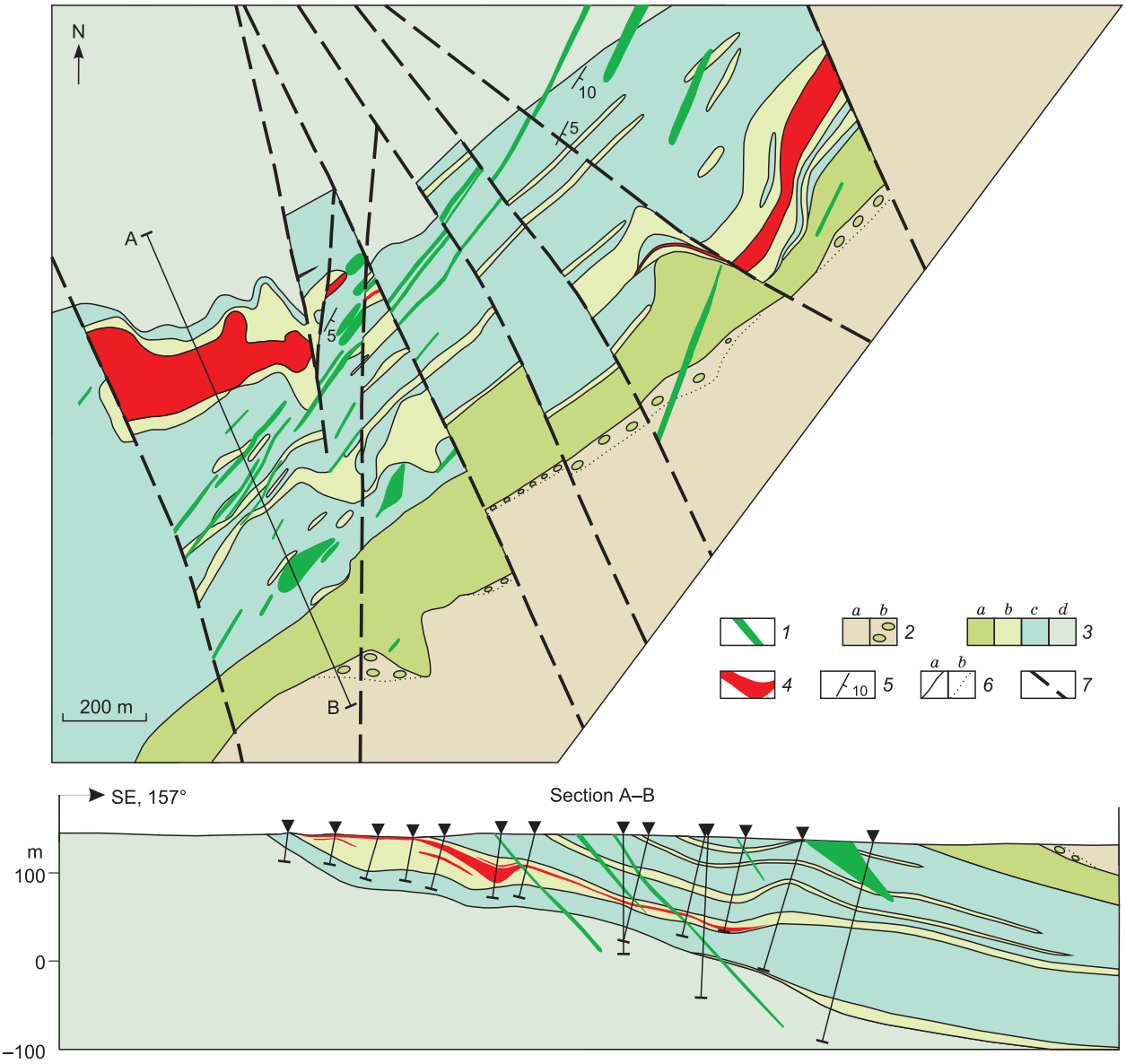

Fig. 6. Scheme of the geologic structure of the Vuruchuaivench low-sulfide PGE deposit and the section A–B, modified from data obtained by V.N. Ivanchenko in 2009. *1*, metadolerite dikes; *2*, Imandra–Varzuga rift structure: metabasalt (*a*), polymict basal conglomerate (*b*); *3*, Vuruchuaivench massif: leuco-mesocratic metagabbro and quartz metagabbronorite (*a*), saussuritized plagioclasite (*b*), mesocratic metagabbronorite (*c*), meso-melanocratic metagabbronorite (*d*); *4*, PGE ore; *5*, dips and strikes; *6*, geologic boundaries: proved (*a*), facies (*b*); *7*, faults.

points of which are located above the general trend because of the higher contents of Ni in the ore (Fig. 9*a*), which is apparently present in both sulfide and silicate forms. The highest correlation between Cu and S has been established for the Western Nittis deposit; a less significant one, for the Moroshkovoe Ozero manifestation; and no correlation, for the other deposits and manifestations (Fig. 9*b*). There is also no correlation between the Pt + Pd contents and the S and Ni contents (Fig. 9*c*, *d*), except for the Western Nittis deposit, in which a high positive correlation of Pt + Pd with S and Ni has been established (Fig. 9*c*, *d*). A high correlation between Pt + Pd and Cu is observed in the Western Nittis deposit, and a weaker one, in the Arvarench manifestation and the OH330 deposit (Fig. 9*e*). In general, there is a positive correlation between the Pt and Pd contents, except for the OH330 deposit and the Nyud manifestation (Fig. 9*f*).

There are clear correlations between the Ni and S contents in the Vuruchuaivench and Southern Sopcha low-sulfide Pt–Pd deposits (Fig. 10*a*) and weaker correlations between the Cu and S contents in the Vuruchuaivench and Loipishnyun deposits (Fig. 10*b*). All low-sulfide deposits show no correlation between Pt + Pd and S (Fig. 10*c*). A high correlation of Pt + Pd with Ni and Cu has been established only in the Vuruchuaivench deposit (Fig. 10*d*, *e*).

Table 4. PGE, Au, Ni, and Cu contents (ppm) in some sulfide PGE–Cu–Ni manifestations and low-sulfide Pt–Pd deposits of the Monchegorsk ore district

Component	Upper reef of Terrasa					Lower reef of Terrasa					Southern Sopcha					Vuruchuaivench			
	425/1	425/2	425/3	425/4	Average	BH-23/77.1	BH-23/79.3	BH-23/80.3	BH-23/82.7	Average	BH-4391/123.8	BH-4391/141.7	BH-4391/143.7	BH-4391/153.5	BH-4391/225.4	Average	419	419/1	Average
Os	0.002	0.001	0.002	0.001	0.002	0.0008	0.0005	0.0009	0.0004	0.001	0.004	0.008	0.005	0.001	0.001	0.004	0.003	0.001	0.002
Ir	0.007	0.007	0.008	0.004	0.007	0.007	0.004	0.005	0.005	0.005	0.013	0.030	0.028	0.003	0.006	0.016	0.012	0.004	0.008
Ru	0.007	0.006	0.008	0.009	0.008	0.004	0.002	0.004	0.004	0.004	0.006	0.015	0.014	0.002	0.002	0.008	0.007	0.002	0.004
Rh	0.071	0.049	0.057	0.025	0.051	0.061	0.026	0.035	0.033	0.039	0.053	0.125	0.107	0.015	0.024	0.065	0.119	0.036	0.078
Pt	0.19	0.16	0.17	0.86	0.35	0.17	0.08	0.10	0.11	0.12	0.68	1.63	1.06	0.10	0.48	0.79	0.64	0.25	0.45
Pd	1.06	1.05	1.34	1.11	1.14	1.21	0.62	0.76	0.77	0.84	1.76	3.40	2.25	0.35	0.89	1.73	5.49	2.07	3.78
ΣPGE	1.337	1.273	1.585	2.009	1.551	1.450	0.736	0.908	0.919	1.003	2.517	5.208	3.464	0.472	1.401	2.613	6.274	2.364	4.319
ΣPPGE/ΣIPGE	83	90	87	143	99	122	112	91	97	106	109	97	72	86	148	94	287	363	325
Au	0.066	0.081	0.104	0.066	0.079	0.066	0.028	0.034	0.040	0.042	0.168	0.186	0.086	0.135	0.148	0.145	0.300	0.019	0.160
Ni	2190	2060	2460	1600	2078	2700	1800	2100	2800	2350	800	3200	700	500	800	1200	3200	800	2000
Cu	1340	1650	1820	940	1438	2100	1700	1800	2200	1950	2800	4900	800	1400	1500	2280	4900	1900	3400

A positive correlation between Pt and Pd is observed in all low-sulfide Pt–Pd deposits, with the highest one being in the Vuruchuaivench deposit (Fig. 10*f*).

The contents of all PGE, Ni, Cu, and Au in some sulfide PGE–Cu–Ni manifestations and low-sulfide Pt–Pd deposits are presented in Table 4, and their distribution is shown in Fig. 11. All the studied deposits and manifestations are characterized by a significant fractionation of PPGE (Pt, Pd, and Rh) relative to IPGE (Os, Ir, and Ru), being the highest in the Vuruchuaivench deposit (Table 4). The PGE patterns of PGE–Cu–Ni ores are broken because of positive Ir and Rh anomalies and negative Ru anomalies (Fig. 11*a*). The positive Ir and Rh anomalies in the absence of their own mineral phases can be explained by their presence as an isomorphic impurity in pentlandite, as was found for the Bushveld Complex (Junge et al., 2015).

The PGE patterns of the Southern Sopcha and Vuruchuaivench low-sulfide deposits are the same as the PGE patterns of sulfide deposits (Karykowski et al., 2018b). The Loipishnyun deposit differs noticeably from them in a less broken pattern because of a slightly pronounced positive Rh anomaly (Fig. 11*b*).

DISCUSSION

Genetic aspects of the formation of the MOD deposits

The concept of the magmatic nature of sulfide Cu–Ni deposits is generally accepted. It implies the formation of such deposits as a result of the segregation of an immiscible sulfide liquid during the cooling of sulfur-saturated mafic and ultramafic magma. Contamination of crustal rocks with mafic magma might have played a crucial role in the saturation of the melt with sulfur, as it increases the limit of sulfide sulfur saturation of melts (Sharkov and Bogatikov, 1998;

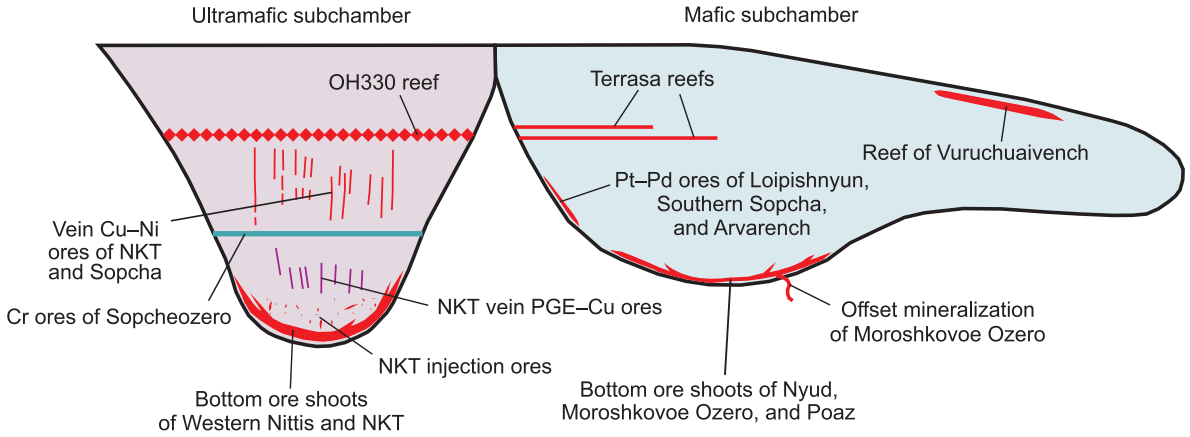

Fig. 7. Model of the localization of sulfide PGE–Cu–Ni and low-sulfide Pt–Pd ores in the layered intrusions of the Monchegorsk ore district.

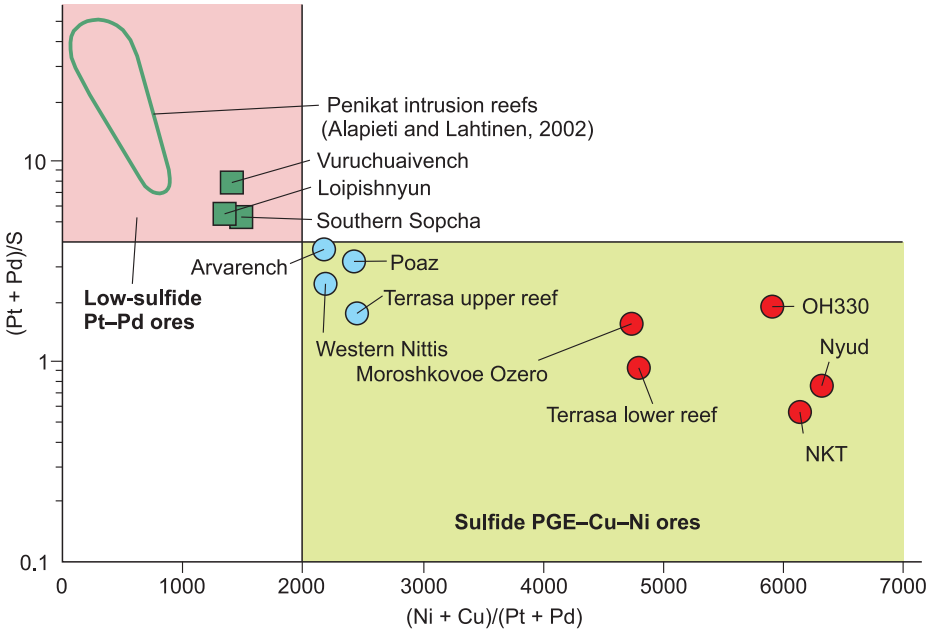

Fig. 8. (Pt + Pd) (ppm)/S (wt.%)–(Ni + Cu)/(Pt + Pd) diagram for the sulfide PGE–Cu–Ni and low-sulfide Pt–Pd deposits and manifestations of the Monchegorsk ore district.

Hutchinson and McDonald, 2008; Naldrett, 2010; Sharman et al., 2013). This concept can be applied to the MOD sulfide PGE–Cu–Ni deposits and manifestations, but the mechanisms of basal- and reef-type ore formation are specific.

The orebodies in the Monchepluton basal-type sulfide PGE–Cu–Ni ores are confined to the lower parts of intrusions and are often spatially associated with altered rocks (metanorite and metaorthopyroxenite), which points to the local addition of water to the magma during the partial melting of the basement (Karykowski et al., 2018a). At the same time, this process can lead to the dilution of the existing PGE-rich sulfide melt (Hutchinson and McDonald, 2008; Sharman et al., 2013). At relatively low contents of Ni, Cu, and S in the parental magma, the localization of sulfide liquid is due to the segregation of PGE-enriched sulfide droplets, which grew, joined together into larger drops and, less often, nests, and settled under gravity into the lower part of the magma chamber (Godel, 2015). They can concentrate to form layers and lenses rich in sulfides upon subsequent separation. In some cases (the Moroshkovoe Ozero manifestation), sulfide liquid was fractionated, became enriched in Cu, and percolated into the basement rocks (Fig. 7). Such migration of sulfide fluid is known in the Sukhanko layered intrusion of the Portimo Complex, where Cu- and PGE-rich sulfide mineralization was found 30 m below the basement of the intrusion (Iljina et al., 2015).

This ore process occurred mainly at R = 3000–5000, a model sulfide content of ca. 5% (Fig. 12*a*), and under moderate fractionation of sulfide liquid (F = 0.25–0.50, Fig. 12*b*), which is consistent with the data of Karykowski et al. (2018a). The low R value reflects a significant amount of sulfides as compared with the host magma, which is sufficient for the formation of Cu–Ni ores at low PGE contents (Godel, 2015). The ore formation parameters in the Western Nittis deposit, Poaz manifestation, and the upper reef of the Terrasa manifestation differ from the above ones: R = 10,000 and the model sulfide content is 2–3% (Fig. 12*a*). They are similar in these features to low-sulfide Pt–Pd deposits (Fig. 8).

Most of sulfide PGE–Cu–Ni ores are characterized by a weak Pt + Pd correlation with S and Ni, except for those of the Western Nittis deposit (Fig. 9*c*). Some ores show a significant correlation between Pt + Pd and Cu (Fig. 9*e*), which is obviously evidence for the sulfide melt fractionation. This assumption is confirmed by the example of the Arvarench manifestation with domination of Cu over Ni (Table 2). The same is evidenced by the wide occurrence of compounds of Pd and, less often, Pt with Te and Bi, in particular, michenerite and merenskyite in the PGE–Cu–Ni ores. These minerals coexist at <500 ºC according to experimental data (Makovicky, 2002).

The Monchepluton reef-type sulfide PGE–Cu–Ni ores (OH330 and Terrasa) are atypical of this type deposits. The OH330 deposit is similar in its position in the Sopcha massif section to the lower sulfide zone of the Great Dyke in Zimbabwe (Wilson et al., 1989; Naldrett and Wilson, 1990; Wilson and Prendergast, 2001) but differs from it in the location in the middle part of orthopyroxenite series and in its smaller thickness. The age of the OH330 orthopyroxenite (2492.5 ± 4.1 Ma) is reliable evidence that the deposit formed later than the Sopcha host rocks as a result of the injection of sulfur-saturated magma. Apparently, the sulfur saturation is due to the contamination of crustal rocks with mafic magma in the intermediate chamber, which is proved by the abnor-

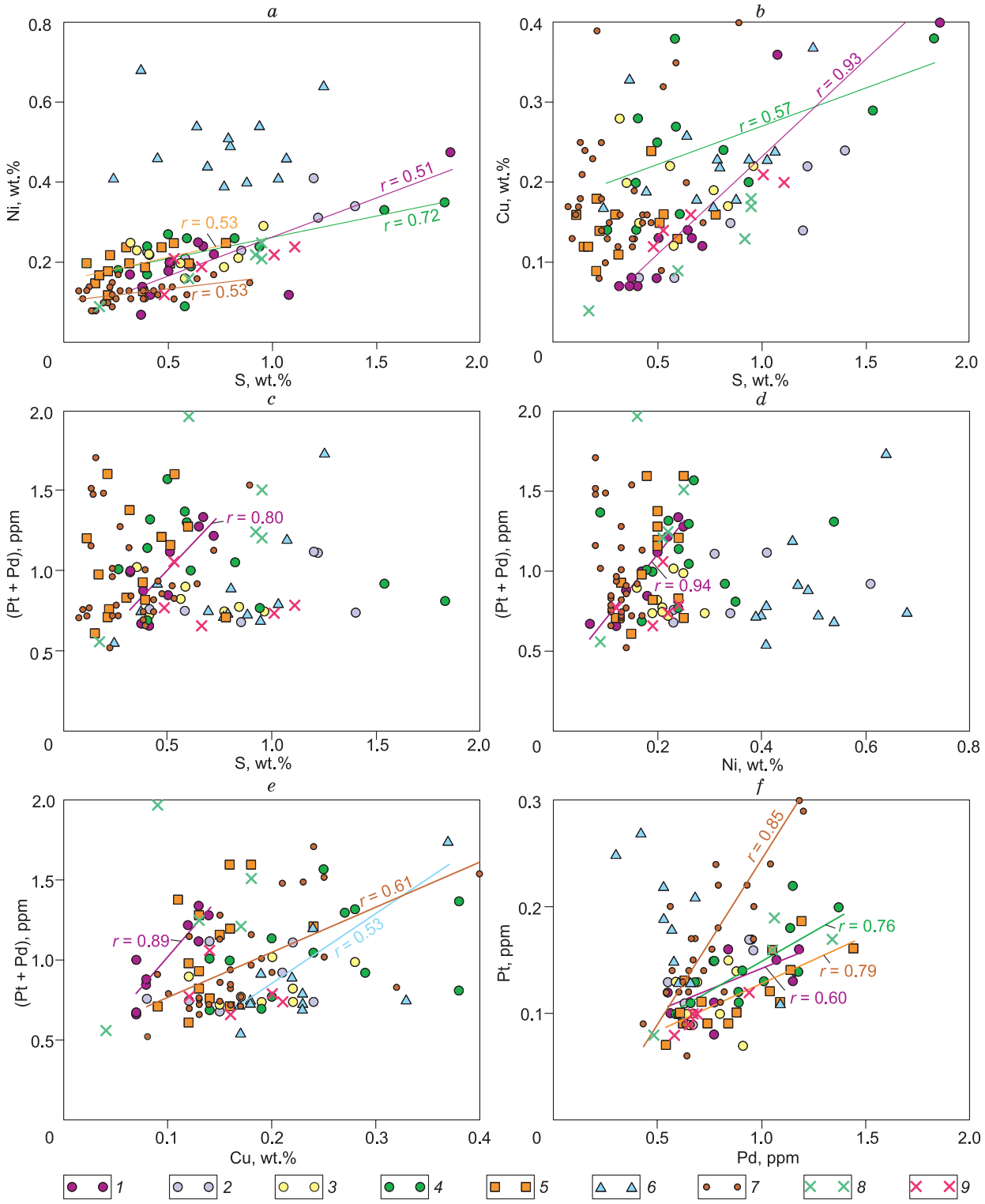

Fig. 9. Binary variation diagrams for chalcophile and siderophile elements of sulfide PGE–Cu–Ni ores (average compositions): Ni–S (*a*), Cu–S (*b*), (Pt + Pd)–S (*c*), (Pt + Pd)–Ni (*d*), (Pt + Pd)–Cu (*e*), and Pt–Pd (*f*). *1–9*, deposits and manifestations: *1*, Western Nittis, *2*, NKT, *3*, Nyud, *4,* Moroshkovoe Ozero, *5*, Poaz, *6*, OH330, *7*, Arvarench, *8–9*, Terrasa: *8*, upper reef, *9*, lower reef. Here and in Fig. 10, the trends and significant correlation coefficients (*r*) are of the same color as the composition points of the deposits and manifestations.

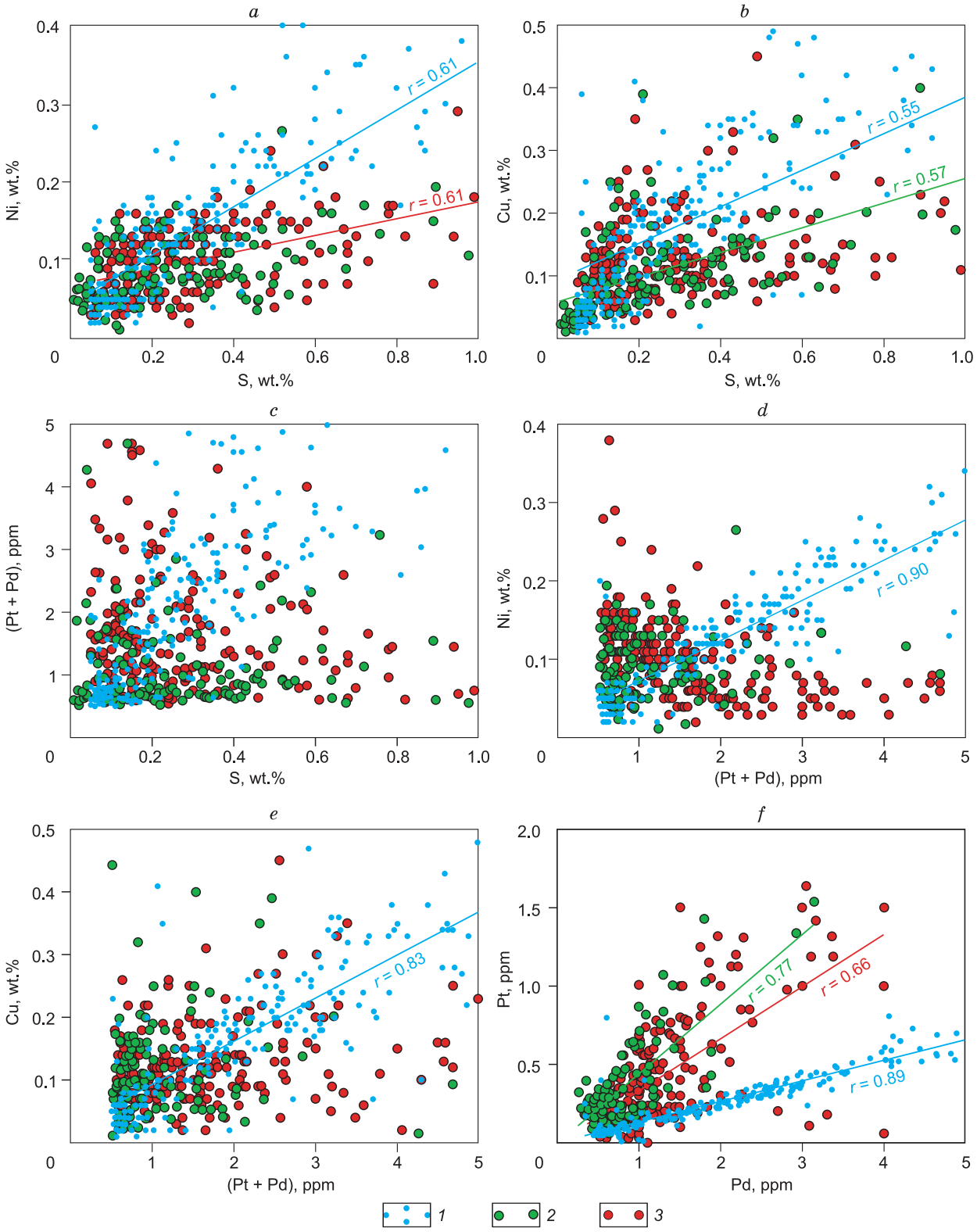

Fig. 10. Binary variation diagrams for chalcophile and siderophile elements of low-sulfide Pt–Pd ores (average compositions): Ni–S (*a*), Cu–S (*b*), (Pt + Pd)–S (*c*), Ni–(Pt + Pd) (*d*), Cu–(Pt + Pd) (*e*), and Pt–Pd (*f*). *1–3*, deposits: *1*, Vuruchuaivench, *2*, Loipishnyun, *3*, Southern Sopcha.

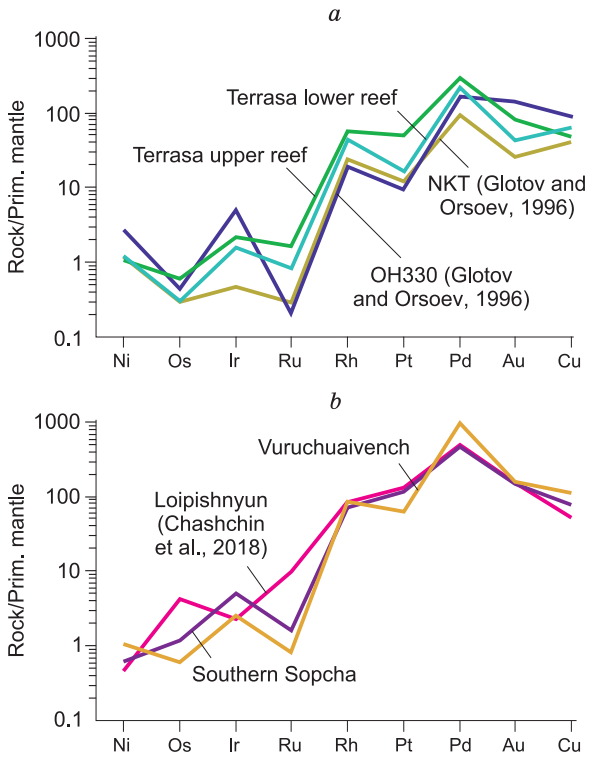

Fig. 11. Primitive-mantle-normalized (McDonough and Sun, 1995) PGE, Au, Ni, and Cu patterns of sulfide PGE–Cu–Ni (*a*) and low-sulfide Pt–Pd (*b*) ores of the Monchegorsk ore district.

mally low Nd isotope ratio in the OH330 harzburgite (Chashchin et al., 2016). The cooling and crystallization of the silicate component contributed to the formation of an immiscible sulfide liquid, which absorbed PGE. These sulfides precipitated to form ore concentrates and PGM, mostly Pt–Fe alloys in harzburgite of the lower part of the OH330 deposit. Later, the residual liquid saturated with fluids and enriched in PGE after the silicate cumulus solidification migrated upward to the horizon of pegmatoid orthopyroxenite, which led to its partial amphibolization and the crystallization of PGM, mainly bismuthide–tellurides.

An alternative model for the OH330 formation was proposed by Karykowski et al. (2018b), who considered this deposit to be the result of the injection of multiphase crystalline mushy melts, some of which contained sulfides. However, the ascent of mushy melt along a thin vertical channel seems unlikely because of its high viscosity and thus could not have been the cause of magma spreading over a near horizontal surface.

The Terrasa manifestation reefs also resulted from the injection of more primitive sulfur-saturated magma into the consolidated Nyud norite. At the same time, the correlations of Pt + Pd with S, Ni, and Cu in the upper and lower reefs are significantly different. The upper-reef ore shows a positive correlation of Pt + Pd with these elements, whereas the lower-reef ore shows no such correlation (Fig. 9*c–e*). This indicates that the PGE concentration in the upper reef is due to the sulfide liquid, as in the OH330 deposit reef, whereas in the lower reef it is, most likely, due to a fluid transfer.

The low-sulfide PGE ore formation proceeded at R = 10,000, a model sulfide content of ca. 1% (Fig. 12*a*), and the high degree of fractionation of the sulfide liquid (F ca. 0.25, Fig. 12*b*). These parameters indicate that the small amount of sulfides was produced in magma chambers at a high concentration of PGE, favorable for the formation of Pt–Pd deposits (Godel, 2015). There is a widely held view of the genesis of low-sulfide Pt–Pd ores (Sharkov and Bogatikov, 1998; Sharkov, 2006; Grokhovskaya et al., 2009), according to which the formation of commercial PGE contents in low-sulfide Pt-Pd ores is the result of complex and multistage mineral-forming processes, beginning from the magmatic stage and ending with hydrothermal–metasomatic transformations.

This is confirmed by the example of the Loipishnyun deposit, where the ore formation proceeded under varying sulfur fugacity (Chashchin et al., 2017), beginning from the late magmatic stage (1000–700 °C), when the crystallization of rock-forming anhydrous silicates led to the separation of residual fluid-saturated intercumulus melt and its migration to the magma chamber top. The subsequent cooling of this melt was accompanied by the crystallization of dark-colored hydrous minerals, base metal sulfides, and PGM localized in the interstices of orthopyroxene cumulates (Chashchin et al., 2017, 2018). The final stage of the ore process (<500 °C) is associated with the dissolution of primary PGM and the formation of secondary compounds enriched in Cu (Chashchin et al., 2018). Such a wide temperature range of platinum-metal ore formation is reflected in significant variations in the PGM composition.

A similar formation mechanism was reported (Knauf and Guseva, 2011) for the Southern Sopcha deposit, which has much in common, first of all, in structural position, with the Loipishnyun deposit. According to the above authors the Southern Sopcha ores are the result of the crystallization of residual melt enriched in ore components and fluids.

The Vuruchuaivench reef-type low-sulfide deposit has specific features: localization in the upper part of the massif section in spatial association with the banding zone, confinement of ore-bearing saussaritized plagioclasite to the taxitic metagabbronorite horizon, domination of Cu over Ni (Table 2), high degree of PGE fractionation (Table 4), and assemblage of PGM with postmagmatic sulfide paragenesis (Grokhovskaya et al., 2000). This deposit is similar in some of these features to the Platinova Reef of the Skaergaard layered intrusion (Nielsen et al., 2005; Andersen, 2006), although their ore-bearing rocks have significantly different compositions. The Vuruchuaivench reef is, most likely, the result of the fractional crystallization of magma of the Monchepluton mafic subchamber and, thus, a significant increase in the concentration of sulfur dissolved in the residual melt. This residual intercumulus melt enriched in fluids and PGE migrated to the top of the subchamber at the final stage of fractionation, causing autometasomatic changes in rock-

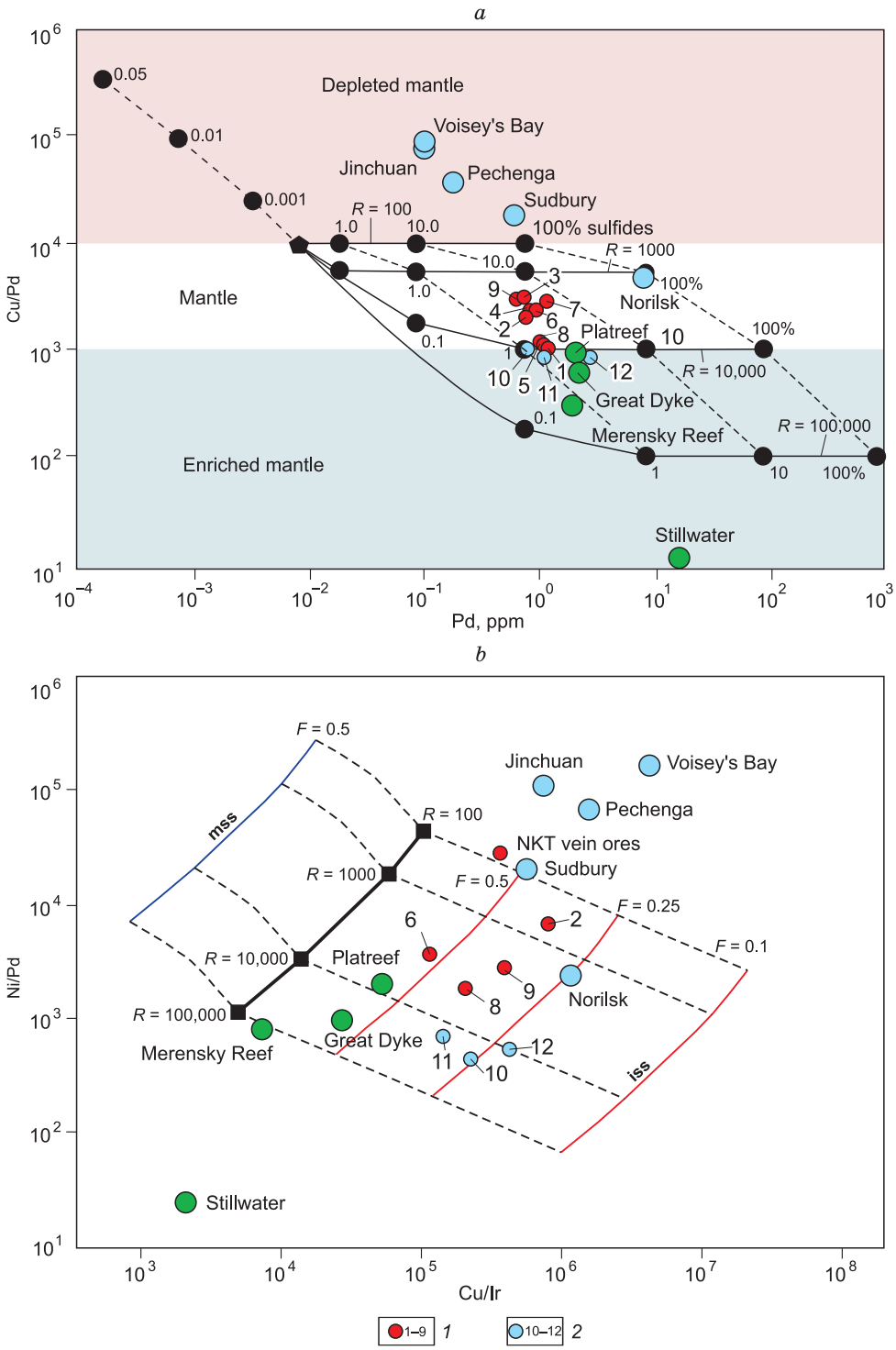

Fig. 12. Cu/Pd–Pd (Barnes et al., 1993) (*a*) and Ni/Pd–Cu/Ir (Karykowski et al., 2018a) (*b*) diagrams for sulfide PGE–Cu–Ni and low-sulfide Pt–Pd ores of the Monchegorsk ore district. *1,* sulfide PGE–Cu–Ni deposites and manifestations: 1, Western Nittis, 2, NKT, 3, Nyud, 4, Moroshkovoe Ozero, 5, Poaz, 6, OH330, 7, Arvarench, 8, upper reef of Terrasa, 9, lower reef of Terrasa; *2*, low-sulfide Pt–Pd deposits: 10, Loipishnyun, 11, Southern Sopcha, 12, Vuruchuaivench. *R*, silicate liquid/sulfide liquid ratio. Position of the world sulfide PGE–Cu–Ni (dark blue circles) and low-sulfide Pt–Pd (green circles) deposits (Naldrett, 2010). In *b*, a solid black line marks the model compositions of sulfides at different *R* values. Black dashed lines mark the compositions of mixtures of monosulfide solid solution (mss) and intermediate sulfide solid solution (iss) at different *R* values. Dark blue line shows the mss composition, and red lines, the compositions of residual sulfide liquid at different degrees of fractionation (*F* is the fraction of residual liquid).

forming silicates and the formation of PGM in assemblage with postmagmatic sulfides.

The predicted PGE potential and prospects for the discovery of new deposits

The MOD is highly promising for increasing the deposit reserves and discovering large commercial PGE deposits based on existing manifestations. In particular, the northeastern flank of the Vuruchuaivench deposit and the Poaz and Arvarench manifestations, where large predicted PGE resources have been revealed, are of great interest for appraisal and exploration work. At the same time, some Monchepluton massifs have been insufficiently studied in terms of the PGE potential. For example, the exploration carried out at small sites of the NKT and Nyud massifs does not give a good impression of the PGE potential of these massifs, and the PGE content of the near-bottom part of the Sopcha massif has not been studied at all.

At present, the total evaluated reserves of Pt + Pd in the MOD deposits are about 200 t, and their predicted resources are estimated at more than 700 t. The geological and economic assessment showed the profitability of exploitation of the MOD PGE deposits and manifestations despite the low average Pt + Pd contents (mostly no more than 1.5 ppm).

The geologic structure of the Monchepluton provides prerequisites for the discovery of reef PGE mineralization in the lower and upper parts of its section. In particular, PGM might be discovered in the zone of orthopyroxenite and harzburgite alternation in the lower part of the NKT and Sopcha massifs, by analogy with the localization of PGE mineralization in the Mirabela (Brazil) (Barnes et al., 2011) and Kapalagulu (Tanzania) (Maier et al., 2008) layered intrusions. The orthopyroxenite zone of the Nittis massif in the upper part of the NKT section is promising for the discovery of a reef PGE deposit, by analogy with the localization of the OH330 deposit. According to the data obtained by V.N. Ivanchenko in 2020, there are also prerequisites for the discovery of reef PGE mineralization in the upper part of the Poaz massif, as was established during the prospecting by AO Rosgeologiya.

Note that the interest in the PGE raw materials of the Kola region has drastically increased in recent time. For example, preparatory work is carried out at the Fedorova Tundra deposit. This is due mainly to the Pd composition of ores and stable high world prices for Pd. Other crucial favorable factors are: the great thickness of ore zones in basal sulfide deposits, the significant length of reef orebodies, the mostly shallow occurrence of deposits, the good ore dressing results, and the low-sulfur composition of ores, which makes a low anthropogenic impact on the environment.

Thus, the MOD layered intrusions contain significant reserves and large predicted resources of sulfide PGE–Cu–Ni and low-sulfide Pt–Pd ores. This puts the MOD in the ranks of one of the world's largest metallogenic taxa with a great potential for PGE ores of various geologic and commercial types.

CONCLUSIONS

The MOD deposits and manifestations of basal and reef-type sulfide PGE–Cu–Ni and low-sulfide Pt–Pd ores are spatially and genetically associated with the Paleoproterozoic (ca. 2.5 Ga) layered intrusions (Monchepluton and Monchetundra massif). The Western Nittis (basal) and OH330 (reef-type) deposits and the NKT, Nyud, Moroshkovoe Ozero, Poaz, Arvarench (basal), and Terrasa (reef) manifestations are of the sulfide PGE–Cu–Ni type. The Loipishnyun, Southern Sopcha (basal), and Vuruchuaivench (reef-type) deposits are of the low-sulfide Pt–Pd type. A specific feature of the basal sulfide deposits is the complex structure of orebodies with impersistent thickness and the uneven distribution of commercial elements, whereas the reef-type deposits are distinguished by a significant extension of orebodies along the strike with a relatively stable thickness.

The sulfides and low-sulfide types of ores differ in PGE mineralogy and geochemical features. In particular, the sulfide PGE–Cu–Ni deposits are characterized mainly by slight variations in PGM composition, whereas the low-sulfide Pt–Pd deposits show PGM assemblages of highly diverse composition. The sulfide PGE–Cu–Ni deposits formed as a result of sulfide immiscibility caused by the contamination of crustal rocks by mafic magmas, the accumulation of base metal sulfides and PGE, and subsequent segregation of ore components in commercial contents. The reef-type OH330 deposit and Terrasa manifestation resulted from the injection of additional portions of sulfur-saturated magma.

The formation of ores in basal low-sulfide Pt–Pd deposits (Loipishnyun and Southern Sopcha) is due to the crystallization of residual melts enriched in ore components and fluids and to subsequent hydrothermal and metasomatic transformations. The reef-type Vuruchuaivench deposit is the result of the deep fractionation of parental magma with the formation of a sulfide liquid enriched in Cu and PGE.

In general, the presence of very large PGE deposits within the MOD and the significant resource potential serve as a reliable mineral resource base for the development of the mining industry in the Kola region of the Arctic western sector.

We thank the reviewers for well-disposed criticism, which helped to improve the paper.

The research was carried out in the framework of project 0226–2019–0053 of the Geological Institute, Apatity. The data on the Western Nittis and Loipishnyun deposits were presented with the consent of ZAO Terskaya Gornaya Kompaniya.

REFERENCES

Alapieti, T.T., Lahtinen, J.J., 2002. Platinum-group element mineralization in layered intrusions of northern Finland and the Kola Peninsula, Russia, in: Cabri, L.J. (Ed.), The Geology, Geochemistry, Mineralogy and Mineral Beneficiation of Platinum-Group Elements. Canadian Institute of Mining, Metallurgy and Petroleum, Montreal, Vol. 54, pp. 507–546.

Alapieti, T.T., Filen, B.A., Lahtinen, J.J., Lavrov, V.V., Smolkin, V.F., Voitsekhovsky, S.N., 1990. Early Proterozoic layered intrusions in the northeastern part of the Fennoscandian Shield. Mineral. Petrol. 42, 1–22, doi: 10.1007/bf01162681.

Amelin, Yu.V., Heaman, L.M., Semenov, V.S., 1995. U–Pb geochronology of layered mafic intrusions in the eastern Baltic Shield: implications for the timing and duration of Paleoproterozoic continental rifting. Precambrian Res. 75 (1–2), 31–46, doi: 10.1016/0301-9268(95)00015-W.

Andersen, J.C.Ø., 2006. Postmagmatic sulphur loss in the Skaergaard intrusion: implications for the formation of the Platinova Reef. Lithos 92, 198–221, doi: 10.1016/j.lithos.2006.03.033.

Balagansky, V.V., Gorbunov, I.A., Mudruk, S.V., 2016. Paleoproterozoic Lapland–Kola and Svecofennian orogens (Baltic Shield). Vestnik KNTs RAN, No. 3, 5–11.

Balashov, Yu.A., Bayanova, T.B., Mitrofanov, F.P., 1993. Isotope data on the age and genesis of layered basic–ultrabasic intrusions in the Kola Peninsula and northern Karelia, northeastern Baltic Shield. Precambrian Res. 64 (1–4), 197–205, doi: 10.1016/0301-9268(93)90076-E.

Barnes, S.-J., Maier, W.D., 2002. Platinum-group element distributions in the Rustenburg layered suite of the Bushveld complex, South Africa, in: Cabri, L.J. (Ed.), The Geology, Geochemistry, Mineralogy and Mineral Beneficiation of Platinum-Group Elements. Canadian Institute of Mining, Metallurgy and Petroleum, Montreal, Vol. 54, pp. 431–458.

Barnes, S.-J., Couture, J.-F., Sawyer, E.W., Bouchaib, C., 1993. Nickel–copper occurrences in the Belleterre–Angliers belt of the Pontiac subprovince and the use of Cu–Pd ratios in interpreting platinum-group element distributions. Econ. Geol. 88, 1402–1418.

Barnes, S.-J., Osborne, G., Cook, D., Barnes, L., Maier, W.D., Godel, B., 2011. The Santa Rita nickel sulfide deposit in the Fazenda Mirabela intrusion, Bahia, Brazil: geology, sulfide geochemistry and genesis. Econ. Geol. 106 (7), 1083–1110, doi: 10.2113/econgeo.106.7.1083.

Bayanova, T.B., Nerovich, L.I., Mitrofanov, F.P., Zhavkov, V.A., Serov, P.A., 2010. The Monchetundra basic massif of the Kola region: new geological and isotope geochronological data. Dokl. Earth Sci. 431 (1), 288–293, doi: 10.1134/S1028334X10030050.

Chashchin, V.V., 1999. Paleoproterozoic complex of layered intrusions of the Kola Peninsula and its metallogeny (Russia). Geol. Ore Deposits 41 (2), 114–125.

Chashchin, V.V., Bayanova, T.B., 2021. The Sopcheozero chromium deposit of the Monchepluton: geochemistry and U–Pb age, in: Proceedings of the Fersman Scientific Session of the Geological Institute of the Kola Science Center [in Russian]. KNTs RAN, Apatity, No. 18, pp. 403–408.

Chashchin, V.V., Mitrofanov, F.P., 2014. The Paleoproterozoic Imandra–Varzuga rifting structure (Kola Peninsula): intrusive magmatism and minerageny. Geodyn. Tectonophys. 5 (1), 231–256.

Chashchin, V.V., Savchenko, Ye.E., 2021a. Ophite gabbronorite at the base of the Kumuzhya massif, Monchepluton: mineralogy, petrogeochemistry, and U–Pb age, in: Proceedings of the Fersman Scientific Session of the Geological Institute of the Kola Science Center [in Russian]. KNTs RAN, Apatity, No. 18, pp. 392–396.

Chashchin, V.V., Savchenko, Ye.E., 2021b. Dunite of the lower zone of the Paleoproterozoic Monchetundra massif: geological and mineralogical-geochemical evidence of the oceanization process, in: Proceedings of the Fersman Scientific Session of the Geological Institute of the Kola Science Center [in Russian]. KNTs RAN, Apatity, No. 18, pp. 397–402.

Chashchin, V.V., Bayanova, T.B., Lyulko, M.S., 2013. Geologic composition and U–Pb age of the Kirikha gabbro-norite massif – Kola Peninsula, Russia, in: Geology and Geochronology of Rock-Forming and Ore Processes in Crystalline Shields. Proceedings of the All-Russian Conference [in Russian]. K & M, Apatity, pp. 179–181.

Chashchin, V.V., Bayanova, T.B., Mitrofanov, F.P., Serov, P.A., 2016. Low-sulfide PGE ores in Paleoproterozoic Monchegorsk pluton and massifs of its southern framing, Kola Peninsula, Russia: Geological characteristic and isotopic geochronological evidence of polychronous ore–magmatic systems. Geol. Ore Deposits 58 (1), 37–57, doi: 10.1134/S1075701516010025.

Chashchin, V.V., Kulchitskaya, A.A., Yelizarova, I.R., 2017. Fluid regime of formation of the Loipishnyun low-sulfide PGE deposit, Monchetundra basic massif (Kola Peninsula, Russia). Litosfera 17 (6), 91–109.

Chashchin, V.V., Petrov, S.V., Drogobuzhskaya, S.V., 2018. Loypishnyun low-sulfide Pt–Pd deposit of the Monchetundra basic massif, Kola Peninsula, Russia. Geol. Ore Deposits 60 (5), 418–448, doi: 10.1134/S1075701518050021.

Chashchin, V.V., Bayanova, T.B., Savchenko, Ye.E., Kiseleva, D.V., Serov, P.A., 2020. Petrogenesis and age of rocks from the lower zone of the Monchetundra mafic platinum-bearing massif, Kola Peninsula. Petrology 28 (2), 151–182, doi: 10.1134/S0869591120020022.

Chashchin, V.V., Petrov, S.V., Kiseleva, D.V., and Savchenko, Ye.E., 2021. Platinum content and formation conditions of the sulfide PGE–Cu–Ni Nyud-II deposit of the Monchegorsk Pluton, Kola Peninsula, Russia. Geol. Ore Deposits 63 (2), 87–117, doi: 10.1134/S1075701521020021.

Dodin, D.A., Chernyshov, N.M., Yatskevich, B.A., 2000. Platinum-Metal Deposits of Russia [in Russian]. Nauka, St. Petersburg.

Gaál, G., Gorbatschev, R., 1987. An outline of the Precambrian evolution of the Baltic shield. Precambrian Res. 35, 15–52, doi: 10.1016/0301-9268(87)90044-1.

Glotov, A.I., Orsoev, D.A., 1996. Distribution of noble metals in the PGE–Cu–Ni–sulfide ores of the Monchegorsk Complex, Kola Peninsula. Dokl. Akad. Nauk 347 (5), 670–673.

Godel, B., 2015. Platinum-group element deposits in layered intrusions: recent advances in the understanding of the ore forming processes, in: Charlier, B., Namur, O., Latypov, R., Tegner, C. (Eds.), Layered Intrusions. Springer, Dordrecht, Heidelberg, New York, London, pp. 379–432.

Gorbunov, G.I., Yakovlev, Yu.N., Goncharov, Yu.V., Gorelov, V.A., Tel'nov, V.A., 1985. Nickel-bearing areas of the Kola Peninsula, in: Copper–Nickel Deposits of the Baltic Shield [in Russian]. Nauka, Leningrad, pp. 27–94.

Green, T., Peck, D., 2005. Platinum group elements exploration: economic considerations and geological criteria, in: Mungall, J.E. (Ed.), Exploration for Platinum-Group Elements Deposits. Mineralogical Association of Canada, Short Course Series, Vol. 35, pp. 247–274.

Grokhovskaya, T.L., Bakaev, G.F., Shelepina, E.P., Lapina, M.I., Laputina, I.P., Muravitskaya, G.N., 2000. PGE mineralization in the Vuruchuaivench gabbronorite massif, Monchegorsk pluton (Kola Peninsula, Russia). Geol. Ore Deposits 42 (2), 133–146.

Grokhovskaya, T.L., Bakaev, G.F., Sholokhnev, V.V., Lapina, M.I., Muravitskaya, G.N., Voitekhovich, V.S., 2003. The PGE ore mineralization in the Monchegorsk magmatic layered complex (Kola Peninsula, Russia). Geol. Ore Deposits 45 (4), 287–308.

Grokhovskaya, T.L., Lapina, M.I., Mokhov, A.V., 2009. Assemblages and genesis of platinum-group minerals in low-sulfide ores of the Monchetundra deposit, Kola Peninsula, Russia. Geol. Ore Deposits 51 (6), 467–485, doi: 10.1134/S107570150906004X.

Grokhovskaya, T.L., Ivanchenko, V.N., Karimova, O.V., Griboedova, I.G., Samoshnikova, L.A., 2012. Geology, mineralogy, and genesis of PGE mineralization in the South Sopcha massif, Monchegorsk Complex, Russia. Geol. Ore Deposits 54 (5), 347–369, doi: 10.1134/S1075701512050029.

Groshev, N.Yu., Rundkvist, T.V., Karykowski, B.T., Maier, W.D., Korchagin, A.U., Ivanov, A.N., Junge, M., 2019. Low-sulfide platinum–palladium deposits of the Paleoproterozoic Fedorova–Pana layered complex, Kola Region, Russia. Minerals 9(12), 764, doi: 10.3390/min9120764.

Gurskaya, L.I., Dodin, D.A., 2015. Mineral resources of platinum group metals in Russia: expansion prospects. Regional'naya Geologiya i Metallogeniya, No. 64, 84–93.

Hutchinson, D., McDonald, I., 2008. Laser ablation ICP-MS study of platinum-group elements in sulfides from the Platreef at Turfspruit, northern limb of the Bushveld Complex, South Africa. Mineral. Deposita 43 (6), 695–711, doi: 10.1007/s00126-008-0190-6.

Iljina, M., Maier, W.D., Karinen, T. 2015. PGE–(Cu–Ni) deposits of the Tornio–Näränkävaara belt of intrusions (Portimo, Penikat, and Koillismaa), in: Maier, W.D., Lahtinen, R., O'Brien, H. (Eds.), Mineral Deposits of Finland. Elsevier, Amsterdam, Oxford, Waltham, pp. 133–164.

Junge, M., Wirth, R., Oberthür, T., Melcher, F., Schreiber, A., 2015. Mineralogical siting of platinum-group elements in pentlandite from the Bushveld Complex, South Africa. Mineral. Deposita 50, 41–54.

Karykowski, B.T., Maier, W.D., Groshev, N.Y., Barnes, S.-J., Pripachkin, P.V., McDonald, I., Savard, D., 2018a. Critical controls on the formation of contact-style PGE–Ni–Cu mineralization: evidence from the Paleoproterozoic Monchegorsk complex, Kola Region, Russia. Econ. Geol. 113 (4), 911–935, doi: 10.5382/econgeo.2018.4576.

Karykowski, B.T., Maier, W.D., Groshev, N.Y., Barnes, S.-J., Pripachkin, P.V., McDonald, I., 2018b. Origin of reef-style PGE mineralization in the Paleoproterozoic Monchegorsk Complex, Kola Region, Russia. Econ. Geol. 113 (6), 1333–1358, doi: 10.5382/econgeo.2018.4594.

Kazanov, O.V., Korneev, S.I., Petrov, S.V., Frolova, A.A., 2016. The distribution of noble metals in the copper–platinum veins of the West Nittis area Monchegorsk layered pluton (Kola Peninsula), in: Problems of Geology and Exploitation of PGE Deposits (First Scientific Readings in Memory of Prof. V.G. Lazarenkov). Proceedings of the All-Russian Conference with International Participation [in Russian]. SPGU, St. Petersburg, pp. 62–65.

Knauf, V.V., Guseva, N.S., 2011. A new formation type of PGE ores in two-member sections of massifs in the southern framing of the Monchegorsk layered pluton, in: Platinum of Russia [in Russian]. Izd. KNIIGiMS, Krasnoyarsk, Vol. 7, pp. 313–329.

Korovkin, V.A., Turyleva, L.V., Rudenko, D.G., Zhuravlev, V.A., Klichnikova, G.N., 2003. Mineral Resources in the Northwest Russian Federation [in Russian]. SPb Kartfabrika VSEGEI, St. Petersburg.

Kozlov, N.E., Ivanov, A.A., Nerovich, L.I., 1990. The Lapland Granulite Belt: Primary Nature and Evolution [in Russian]. KNTs RAN, Apatity.

Kozlov, N.E., Sorokhtin, N.O., Glaznev, V.N., Kozlova, N.E., Ivanov, A.A., Kudryashov, N.M., Martynov, E.V., Tyuremnov, V.A., Matyushkin, A.V., Osipenko, L.G., 2006. Geology of the Archean Baltic Shield [in Russian]. Nauka, St. Petersburg.

Krivolutskaya, N.A., Smol'kin, V.F., Svirskaya, N.M., Mamontov, V.P., Fanygin, A.S., Belyatskii, B.V., Roshchina, I.A., 2010. Geochemical features of the drusite massifs, the central part of the Belomorian mobile belt: I. Distribution of major and trace elements in the rocks. Geochem. Int. 48 (5), 465–491, doi: 10.1134/S0016702910050046.

Maier, W.D., 2015. Geology and petrogenesis of magmatic Ni–Cu–PGE–Cr–V deposits: An introduction and overview, in: Maier, W.D., Lahtinen, R., O'Brien, H. (Eds.), Mineral Deposits of Finland. Elsevier, Amsterdam, Oxford, Walrtham, pp. 73–92.

Maier, W.D., Barnes, S.-J., Bandyayera, D., Livesey, T., Li, C., Ripley, E., 2008. Early Kibaran rift-related mafic–ultramafic magmatism in western Tanzania and Burundi: Petrogenesis and ore potential of the Kapalagulu and Musongati layered intrusions. Lithos 101, 24–53, doi: 10.1016/j.lithos.2007.07.015.

Makovicky, E., 2002. Ternary and quaternary phase systems with PGE, in: The Geology, Geochemistry, Mineralogy and Mineral Beneficiation of Platinum-Group Elements. Canadian Institute of Mining, Metallurgy and Petroleum, Montreal, Vol. 54, pp. 131–175.

McDonough, W.F., Sun, S.-S., 1995. The composition of the Earth. Chem. Geol. 120, 223–253, doi: 10.1016/0009-2541(94)00140-4.

Mints, M.V., Glaznev, V.N., Konilov, A.N., Kunina, N.M., Nikitichev, A.P., Raevsky, A.B., Sedykh, Yu.N., Stupak, V.M., Fonarev, V.I., 1996. The Early Precambrian of the Northeastern Baltic Shield: Paleogeodynamics, Crustal Structure and Evolution [in Russian]. Nauchnyi Mir, Moscow.

Mitrofanov, F.P., Smolkin, V.F. (Eds.), 2004. Layered Intrusions of the Monchegorsk Ore District: Petrology, Mineralization, Isotopy, and Deep Structure [in Russian]. KNTs RAN, Apatity.

Mitrofanov, F.P., Balagansky, V.V., Balashov, Yu.A., Gannibal, L.F., Dokuchaeva, V.S., Nerovich, L.I., Radchenko, M.K., Ryungenen, G.I., 1993. The U–Pb age of gabbro–anorthosite massifs of the Kola Peninsula. Dokl. Akad. Nauk 331 (1), 95–98.

Mitrofanov, F.P., Balabonin, N.L., Bayanova, T.B., Korchagin, A.U., Latypov, R.M., Osokin, A.S., Subbotin, V.V., Karpov, S.M., Neradovsky, Yu.N., 1999. The Kola PGE-bearing province: new data, in: Platinum of Russia. The Problems of the Development of the PGE Mineral Resources Base in the 21st Century [in Russian]. ZAO Geoinformmark, Moscow, pp. 43–52.

Naldrett, A.J., 2003. Magmatic Sulfide Deposits of Nickel–Copper and Platinum-Metal Ores [Russian translation]. SPbGU, St. Petersburg.

Naldrett, A.J., 2010. Secular variation of magmatic sulfide deposits and their source magma. Econ. Geol. 105 (3), 669–688, doi: 10.2113/gsecongeo.105.3.669.

Naldrett, A.J., Wilson, A.H., 1990. Horizontal and vertical variations in noble-metal distribution in the Great Dyke of Zimbabwe: a model for the origin of the PGE mineralization by fractional segregation of sulfide. Chem. Geol. 88 (3–4), 279–300, doi: 10.1016/0009-2541(90)90094-N.

Neradovsky, Yu.N., Rundkvist, T.V., Galkin, A.S., Klimentev, V.N., 2002. To the problem of the Sopcha "horizon-330" PGE bearing and its industrial use (the Monchegorsk Pluton). Vestnik MGTU 5 (1), 85–90.

Nerovich, L.I., Bajanova, T.B., Savchenko, E.E., Serov, P.A., Yekimova, N.A., 2009. New data on geology, petrography, isotope geochemistry and PGE mineralization of the Monchetundra intrusion. Vestnik MGTU 12 (3), 461–477.

Nielsen, T.F.D., Andersen, J.C.Ø., Brooks, C.K., 2005. The Platinova Reef of the Skaergaard intrusion, in: Mungall, J.E. (Ed.), Exploration for Platinum Group Element Deposits. Mineralogical Association of Canada, Short Course 35, pp. 431–455.

Rundkvist, T.V., Bayanova, T.B., Sergeev, S.A., Pripachkin, P.V., Grebnev, R.A., 2014. The Paleoproterozoic Vurechuaivench layered Pt-bearing pluton, Kola Peninsula: new results of the U–Pb (ID-TIMS, SHRIMP) dating of baddeleyite and zircon. Dokl. Earth Sci. 454 (1), 1–6, doi: 10.1134/s1028334x14010048.

Sharkov, E.V., 2006. Formation of Layered Intrusions and Associated Mineralization [in Russian]. Nauchnyi Mir, Moscow.

Sharkov, E.V., Bogatikov, O.A., 1998. Concentration mechanisms of the platinum-group elements in layered intrusions of the Kola–Karelia region. Geol. Ore Deposits 40 (5), 372–390.

Sharkov, E.V., Bogatikov, O.A., Krasivskaya, I.S., 2000. The role of mantle plumes in the early Precambrian tectonics of the eastern Baltic Shield. Geotectonics 34 (2), 85–105.

Sharkov, E.V., Krasivskaya, I.S., Chistyakov, A.V., 2004. Dispersed mafic–ultramafic intrusive magmatism in Early Paleoproterozoic mobile zones of the Baltic Shield: An example of the Belomorian drusite (coronite) complex. Petrology 12 (6), 561–582.

Sharman, E.R., Penniston-Dorland, S.C., Kinnaird, J.A., Nex, P.A.M., Brown, M., Wing, B.A., 2013. Primary origin of marginal Ni–Cu–(PGE) mineralization in layered intrusion: $D^{33}S$ evidence from the Platreef, Bushveld, South Africa. Econ. Geol. 108 (2), 365–377, doi: 10.2113/econgeo.108.2.365.

Slabunov, A.I., Balagansky, V.V., Shchipansky, A.A., 2021. Mesoarchean to Paleoproterozoic crustal evolution of the Belomorian province, Fennoscandian Shield, and the tectonic setting of eclogites. Russ. Geol. Geophys. 62 (5), 525–546, doi: 10.2113/RGG20204266.

Sluzhenikin, S.F., Distler, V.V., Dyuzhikov, O.A., Kravtsov, V.F., Kunilov, V.E., Laputina, I.I., Turovtsev, D.M., 1994. Low-sulfide platinum mineralization in the Norilsk differentiated intrusions. Geologiya Rudnykh Mestorozhdenii 36 (3), 195–217.

Sluzhenikin, S.F., Yudovskaya, M.A., Stephen, J., Barnes, S.J., Abramova, V.D., Le Vaillant, M., Petrenko, D.B., Grigor'eva, A.V., Brovchenko, V.D., 2020. Low-sulfide platinum group element ores of the Norilsk–Talnakh camp. Econ. Geol. 115 (6), 1267–1303, doi: 10.5382/econgeo.4749.

Smolkin, V.F., Kremenetsky, A.A., Vetrin, V.R., 2009. Geological and genetic model of the formation of Paleoproterozoic ore-magmatic systems of the Baltic Shield. Otechestvennaya Geologiya, Issue 2, 54–62.

Wilson, A.H., Prendergast, M.D., 2001. Platinum-group element mineralization in the Great Dyke, Zimbabwe, and its relationship to magma evolution and magma chamber structure. S. Afr. J. Geol. 104, 319–342, doi: 10.2113/104.4.319.

Wilson, A.H., Naldrett, A.J., Tredoux, M., 1989. Distribution and controls of platinum group element and base metal mineralization in the Darwendale subchamber of the Great Dyke, Zimbabwe. Geology 17, 649–652, doi: 10.1130/0091-7613(1989)017<0649:DACOPG>2.3.CO;2.